Co-operative Programme for Monitoring and Evaluation of the Long-Range Transmission of Air Pollutant in Europe

EMEP

LONG-RANGE TRANSPORT OF SELECTED POPs

Part II

Physical-chemical properties of dioxins and furans and factors influencing the transport and accumulation of Persistent Organic Pollutants

EMEP/MSC-E Report 2/98

August 1998

METEOROLOGICAL SYNTHESIZING CENTRE - EAST

Kedrova str.8-1, Moscow, 117 292, Russia
Tel.: 007 095 124 47 58
Fax: 007 095 310 70 93
e-mail: msce@glasnet.ru

Introduction

Part II of the report “Long-range transport of selected POPs” deals with consideration of physical-chemical properties of persistent organic pollutants and factors affecting the transport and accumulation of these pollutants in different compartments. In Part I we discussed modelling results of lindane, PCB and B(a)P transport. The other pollutants, included in the Protocol on Persistent Organic Pollutants, are furans and dioxins. For the evaluation of their transport a detail review of their physical-chemical properties was made. These results are used for model parametrization.

One of the most important factors influencing the transport and exchange of POP between compartments is vegetation. A special section of this report is dedicated to the interaction of the atmosphere and vegetation. An attempt is made to reveal the interrelation of POP concentration in the atmosphere and their accumulation and degradation in plants.

To a great extent POP distribution on the global and regional levels are affected by sea currents and accumulation of these species in deep waters. A concise survey of spatial and temporal characteristics of ocean currents within EMEP region was made. It is planned to use these data in the future modelling.

Contents

Chapter 1 Review of physical-chemical properties of polychlorinated dibenzo-p-dioxins (PCDDs) and dibenzofurans (PCDFs) in respect to their longe-range transport in the atmosphere 5

A.A.Bulgakov, D.A.Ioannisian

1. **Introduction** 5
2. **PCDD/Fs emissions to the atmosphere** 6
3. **PCDD/Fs concentration and deposition** 10
- 3.1 PCDD/Fs concentration in the atmosphere 10
- 3.2 PCDD/Fs concentration in soils 11
- 3.3 PCDD/Fs concentration in natural waters 11
- 3.4 PCDD/Fs deposition 11

4. **Parameters of PCDD/Fs migration and degradation in the environment** 14
- 4.1 Melting and boiling points 14
- 4.2 Solubility in water 15
- 4.3 Vapour pressure 17
- 4.4 Henry law constant 18
- 4.5 Partition coefficients in soil and bottom sediments 20
- 4.6 PCDD/Fs gas-aerosol partition 20
- 4.7 PCDD/Fs degradation in the environment 22
- 4.7.1 Degradation in the atmosphere 22
- 4.7.2 Degradation in natural waters 23
- 4.7.3 Degradation in soil 25

5. **Conclusions** 25

References 27

Appendix A 31

Chapter 2 Accumulation of persistent organic pollutants by vegetation 36

B.N.Moisseev

Preface 36

Introduction 36

1. **Methodological approach** 37
2. **Analysis of data of background monitoring stations** 38
- 2.1 Correlation and regression analysis 39
- 2.2 POP long-term accumulation in the green mass of plants 41

3. **Model calculation** 42

3.1 Assimilation of gaseous POP from the atmosphere 42
3.2 POP root uptake 45
3.3 Approximative estimates of POP degradation in plants 46
3.4 Model errors and uncertainties 47
Conclusions 48
Glossary of some biological terms 49
References 50
Annex A 52

Chapter 3 Construction and description of climatological current fields in the upper ocean layer for transport models 60

A.A.Zelenko, Yu.D.Resnyansky, L.K.Erdman

Introduction 60
1 **General information on sea currents** 61
2 **Methods of determination of sea currents** 62
2.1 Direct methods 63
2.2 Indirect methods 63
2.3 Dynamic method of current calculations 64
3 **Source data and procedure for calculation of climatological currents within the EMEP domain using the dynamic method** 65
3.1 Computational domain and the EMEP grid 65
3.2 Source of hydrographic data 65
3.3 Transformation of data and calculations of geostrophic currents 66
3.4 Files of numerical values of current velocities and sea surface temperatures (SST) 66
4 **Basic peculiarities of climatological currents and sea surface temperature in the EMEP domain** 68
5 **Assessments of passive pollutant transport between the upper mixed layer and lower ocean layers** 69
5.1 Ordered vertical motions 69
5.2 Vertical motions in geostrophic currents 69
5.2.1 Vertical motions in drift currents (Ekman pumping) 70
5.2.2 Vertical motions in coastal zones 71
5.3 Turbulent diffusion 71
References 72

Chapter 1 Review of physical-chemical properties of polychlorinated dibenzo-p-dioxins (PCDDs) and dibenzofurans (PCDFs) in respect to their longe-range transport in the atmosphere

A.A.Bulgakov, D.A.Ioannisian

1. Introduction

The objective of the present work is the assessment of physico-chemical parameters for simulation of atmospheric transport of polychlorinated dibenzo-p-dioxin (PCDDs) and dibenzofuran (PCDFs) congeners.

The PCDDs and PCDFs are two groups of tricyclic planar aromatic compounds. They are nonpolar, poorly water-soluble, lipophilic chemicals. Due to planarity they can selectively and very strongly block so-called Ah-receptor - the key link of immune-enzyme system of the living beings. PCDD/Fs reinforce the impact of carcinogens, toxic substances and allergens. That is why they act as an alien hormone and there is no so low concentration that would be safe. PCDD/Fs destroy soil ecosystems that result in soil bacteria mutations, crop capacity decrease, accumulation of soil rots etc. [*Yufit et. al*, 1997].

Structures of PCDDs and PCDFs are shown in Figure 1.1 and 1.2 (numbers indicate the possible chlorine atom positions).

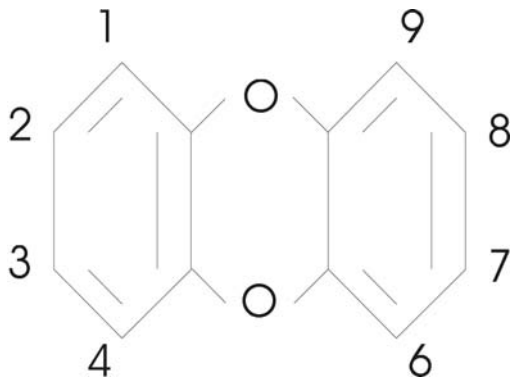

Figure 1.1 Structure of polychlorinated dibenzo-p-dioxins (PCDDs)

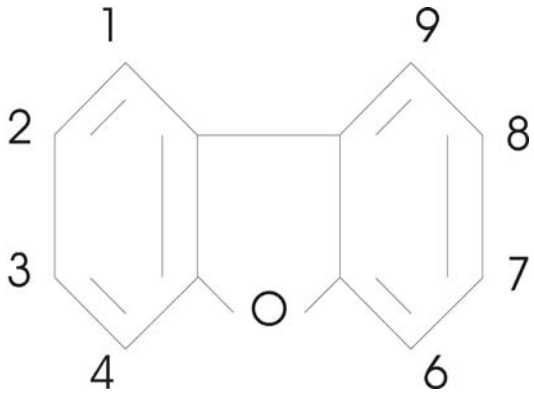

Figure 1.2 Structure of polychlorinated dibenzofurans (PCDFs)

There are 75 PCDD and 135 PCDF isomers in the total with a different number of chlorine atoms and positions in the molecule. Only 7 PCDD and 10 PCDF (congeners containing chlorine atoms in 2,3,7,8 positions) are toxic. According to NATO/CCMS International Toxicity Equivalency Factor (I -TEF) method of risk assessment for complex mixtures of dioxins and related compounds [*International,* 1988] I-TEF of the most toxic 2378-TCDD is assumed to be 1. I-TEF values of PCDD/PCDFs are shown in Table 1.1.

Table 1.1 International Toxicity Equivalency Factor (I–TEF) values of PCDDs and PCDFs [*International*, 1988]

Compound	I -TEF value
2378-TCDD	1
12378-PeCDD	0.5
123478-HxCDD	0.1
123678-HxCDD	0.1
123789-HxCDD	0.1
1234678-HpCDD	0.01
OCDD	0.001
2378-TCDF	0.1
12378-PeCDF	0.05
23478-PeCDF	0.5
123478-HxCDF	0.1
123678-HxCDF	0.1
123789-HxCDF	0.1
234678-HxCDF	0.1
1234678-HpCDF	0.01
1234789-HpCDF	0.01
OCDF	0.001

The following formula is used for determination of toxic equivalent (TEQ) of a mixture:

TEQ = I-TEF·(PCDD/F congener concentration in mixture). Sum of all TEQ gives the total mixture toxicity in TEQ units. The ratio of TEQ to total mass of PCDD/F depends on the congener distribution but usually it is about 1:60 [*Thomas and Spiro*, 1996].

2. PCDD/Fs emissions to the atmosphere

PCDD/Fs formation and input to the environment is connected with two different processes: chlorination of organic compounds and combustion of organic compounds in presence of chlorine-containing products. PCDD/Fs formation in biological processes is impossible, therefore forest and steppe fires and probably volcanoes are the only natural sources of PCDD/Fs.

Chlorination of organic compounds is carried out by the enterprises of chemical (oil processing) industries manufacturing different products, mainly pesticides and polychlorobiphenyls. In this case PCDD/Fs input to the environment can be made both by chemical enterprises and in sites of application of products containing PCDD/Fs. PCDD/Fs formation in combustion processes depends first of all on flame temperature and presence of available chlorine. PCDD/Fs synthesis

and thermal destruction are two competitive reactions in the flame. Synthesis requires sufficiently high temperature for the formation of free chlorine atoms out of initial chlorine-containing products. However, the probability of PCDD/Fs thermal destruction significantly increases with temperature increase. The temperature range of 600-900^{0}C is the optimum for PCDD/Fs formation. Chlorine is a widely spread element in natural fuels and its content varies from trace quantities in natural gas to shares of percent in coal. Chlorine content may be high in some types of plastic (e.g. polychlorovinyl). Thus PCDD/Fs formation intensity depends on composition of combusted material as well.

Reliable estimate of PCDD/Fs emission factors for different anthropogenic sources is complicated by two circumstances. Firstly, methods of PCDD/Fs analysis are extremely complex and expensive. As a rule, reliability of the experimental data is rather low. Secondly, emission factors considerably vary even within one source category and depend on technological characteristics of a specific unit.

Data on emission factors for different source categories and their variation are presented in table 2.1 based on papers [*Holoubec et al*., 1993; *Parma et al.,* 1995; *Atmospheric Emission Inventory Guidebook,* 1996; *Brzuzy and Hites*, 1996; *Berdowski et al.,* 1997; *Douben*, 1997]. The maximum values of emission factors are typical for waste (especially medical) incineration. It is due to a considerable content of different plastics in waste (in medical waste – polychlorovinyl tubes). Since the process temperature is an important factor, in modern waste incinerators (especially, incinerators of hazardous waste) high flame temperature is sustained, thereby reducing emission factors.

Table 2.1 Emission factors for PCDD/Fs

Process	Emission factor, μg I-TEQ/t
Fuel combustion for electricity and heat generation	
Coal	<0.1 – 200
Oil fuel	1 – 20
Natural gas	0.5
Peat	0.1 – 10
Wood	1 – 500
Municipal/medical/industrial waste incineration	0.2 – 4700
Iron and steel production	0.02 – 35
Coke production	0.3
Sinter production	1 – 9
Non-ferrous metal production	5 – 35
Secondary copper production	20 – 650
Secondary aluminum production	130
Gasoline and diesel fuel combustion by transport	0.006 - 60

According to estimates of *J.Berdowski et al.* [1997] the main contribution to PCDD/Fs emissions to the atmosphere in Europe makes combustion of different fuels for heat and electricity generation. Waste incineration is another important source. Data on input of main source

categories to the total PCDD/Fs emission in the EMEP region are presented in table 2.2 [*Berdowski et al.,* 1997].

Table 2.2 Percentage contribution of main source categories to PCDD/Fs emissions to the atmosphere in Europe

Source category	Contribution, %
Stationary fuel combustion for electricity and heat generation	38
Waste incineration	24
Iron and steel industry	17
Non-ferrous metal industry	14
Transport	1
Other	6

It is no doubt that percentage contribution of different source categories is country-to-country variable and depends on the level of development of different industry brunches, used technologies and emission reduction measures.
Estimates of PCDD/Fs emissions for European countries have been made by *J. Berdowski et al*. [1997]. These data are summarized in table 2.3. The total emission within the EMEP grid is estimated to be about 11 kg I-TEQ. The authors are of opinion that uncertainty in emission estimates can exceed an order of magnitude. It is due to a wide range of emission factor variations as well as low reliability of relevant activity statistics. Table 2.3 also presents UN/ECE reported official emission data.

Figure 2.1 presents spatial distribution of PCDD/Fs emissions over 50x50 km^2 EMEP grid [*Berdowski et al.,* 1997]. As follows from the figure the intensity of PCDD/Fs emissions over Europe is highly non-uniform.

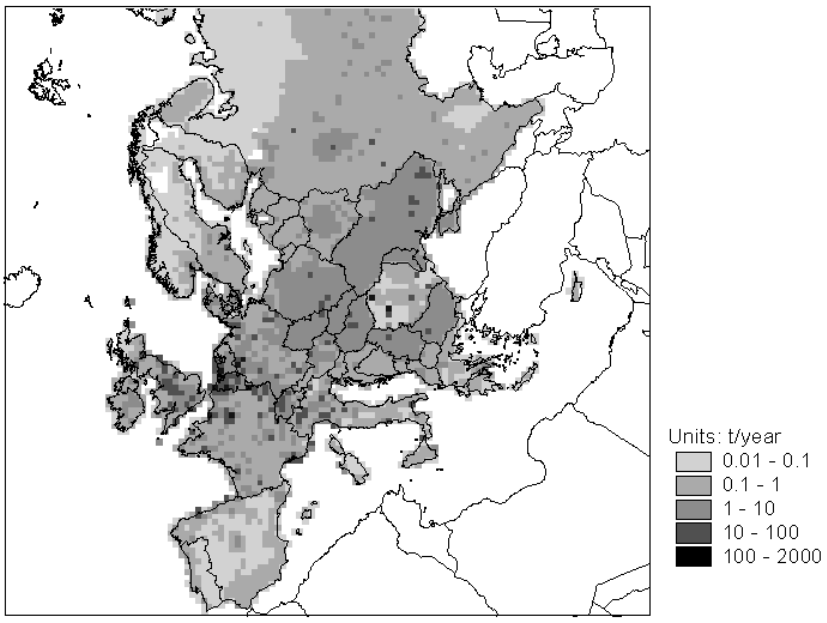

Figure 2.1 Spatial distribution of PCDD/Fs emissions over 50x50 km^2 EMEP grid. Units: t/year

Table 2.3 Emission data of dioxins and furans (g I-TEQ /y)

Country	Estimates for 1990 [*Berdowski et al.*, 1997]	UN/ECE reported official emission data [EB.AIR/GE.1/1997/3; EB.AIR/GE.1/1997/3/Add.1]					
		1990	1991	1992	1993	1994	1995
Albania	12.1						
Austria	84.8					28.7	
Belarus	106						
Belgium	616						426[1)]
Bosnia&Herzegovina	9.35						
Bulgaria	154	554.2					456
Croatia	12.9	2.435					
Cyprus	1.02						
Czech Republic	224						
Denmark	70.6						
Estonia	17.7						
Finland	53.3						155
France	1636	1640					
Germany	1196	1210					
Greece	25.4						
Hungary	167	167.4	158.9	120.8	119.6	113.5	
Iceland	0.553						
Ireland	43.9						
Italy	583						
Latvia	13.5						
Lithuania	23.0						
Luxembourg	27.6						
The FYR of Macedonia	4.90						
Republic of Moldova	22.7						
Netherlands	505	618		505			
Norway	38.7						
Poland	359	359					368
Portugal	17.4						
Romania	1500						
Russian Federation[2)]	1020						
Slovakia	43.0						
Slovenia	5.99						
Spain	134	133.8					
Sweden	83.5	58-127			19-46		
Switzerland	242	242	230	217	203	192	181
Ukraine	877						
United Kingdom	881				800		
Yugoslavia	112						
Total	10924						

[1)] this value represents the sum for the Wallonie and Flanders regions; [2)] European part

3. PCDD/Fs concentration and deposition

3.1 PCDD/Fs concentration in the atmosphere

Published values of PCDD/Fs concentrations in the atmospheric air are summarised in Table A1 (Appendix A). Typical concentrations in urban areas in Europe and USA range from 0.05 to 1 pg TEQ/m^3. The upper limit of this interval refers to sampling points in the proximity of pollution sources. Typical concentrations in rural areas range from 0.01 to 0.1 pg TEQ/m^3. Urban air PCDD/Fs concentrations are usually 4-6 times higher than rural concentrations in the same region [*Lorber et al*., 1994].

Tables A2 and A3 (Appendix A) summarise available data on PCDD/F homologue pattern and percent contribution of the 2378-substituted congeners to their homologue group in the atmospheric air. PCDD/F homologue pattern and percent contribution of the 2378-substituted congeners to each homologue group in suburban and urban air samples from different sites are very similar and close to that in the proximity of the pollution sources (municipal waste incinerators (MWI) and motorway tunnels). Standard deviations of averaged percentage of homologue groups content in the total concentration of atmospheric PCDD/Fs are 50% or less for all groups of environmental interest. A significant or even prevailing part of this variability can be explained by uncertainties of experimental determination of PCDD/Fs isomers. It indicates that the homologue pattern of PCDD/Fs in urban and suburban air can be probably estimated to appropriate accuracy.

Contribution of PCDD/Fs homologue groups to the total concentration in the atmospheric air in urban area was estimated using data from tables 1.1 and A2, A3 (Appendix A). The results are presented in table 3.1:

Table 3.1 Percentage contribution of PCDD/Fs homologue groups to the total concentration in urban area

Homologue group	Contribution, %
TCDF	4.5
PeCDF	30
HxCDF	21
HpCDF	2.6
OCDF	0.2
TCDD	3.7
PeCDD	13
HxCDD	18
HpCDD	5.4
OCDD	1.3

Thus, the contribution of PeCDD/Fs and HxCDD/Fs is more than 80% while the input of the rest homologue groups is less than 20%.

PCDD/Fs concentrations in the atmospheric air vary with seasons. Winter concentrations are higher than summer ones by factors varying between 1.1 and 9 [*Jones and Duarte-Davidson*, 1997; *Hippellein et al*., 1996; *Fiedler,* 1996]. There are also evidences of decrease of PCDD/F mean annual concentrations in the atmosphere during the last years [*Fiedler*, 1996].

3.2 PCDD/Fs concentration in soils

Data on PCDD/Fs concentrations in soils are summarised in Table A4 (Appendix A). Vertical distribution of PCDD/F in soils is non-uniform [*Brzuzy and Hites*, 1995]. Thus, results of soil concentration determination for these contaminants depend on the depth of sampling. Unfortunately, some researchers do not report on the depth of sampled soil layer (see Table A4 (Appendix A)). Another problem is that soil concentrations are calculated on the base of dry or wet weight of soil and reported in pg/g or in pg TEQ/g.. Concentrations based on dry and wet weight of soil can be converted into each other without significant error, but conversion of soil concentrations expressed in terms of pg/g into concentrations in pg TEQ/g requires additional data on congener-specific composition of the contamination. Different accumulation and stability of PCDD/Fs congeners in soil lead to a pronounced site-to- site variation of their homologue pattern (see Table A5 (Appendix A)). A homologue group percentage differs by a factor of 100 even for two sites in the same city [*Creaser et al*., 1990]. For this reason concentration in pg/g does not correspond to concentration in pg TEQ/g appropriately.

The above-mentioned problems complicate significantly the comparison of data obtained in different studies and given in Table A4 (Appendix A). The only conclusion can be made is that PCDD/Fs concentrations in soil normally decrease with distance from the centre of urban area [*Broman et al*., 1990; *Creaser et al*., 1990]

3.3 PCDD/Fs concentration in natural waters

According to *R.Duarte-Davidson et al*. [1997] typical PCDD/Fs concentration in river water of UK is 3.5 pg/l or 38 pg TEQ/m^3. The mean concentration of PCDD/Fs in Japanese ponds is 261 pg/l [*Matsuda et al*., 1997]. PCDD/Fs concentrations in seawater (Seto Inland Sea, October 1994) ranged from 8.3 to 168.2 pg/l [*Matsuda et al*., 1997].

3.4 PCDD/Fs deposition

Data on PCDD/Fs deposition velocities (deposition flux-to-air concentration ratio) and deposition fluxes from the atmosphere are summarised in Table 3.2. Experimentally measured deposition fluxes in rural areas are about 10 pg TEQ/m^2 per day, in urban areas - n×10 pg TEQ/m^2 per day in the vicinity of a point source - n×100 pg TEQ/m^2 per day, where n = 1-10.

Table 3.2 PCDD/Fs deposition

Site and sampling period	Deposition velocity, cm/s	Deposition flux, mean and range, pg TEQ/m^2 day	Reference
Bolsover, UK, 6 km from the industrial complex, October 1992-October 1993	0.27	23 (3-70)	*Jones and Duarte-Davidson*, 1997
Bolsover, UK, 2 km from the industrial complex, October 1992-October 1993	-	21 (2-54)	
Bolsover, UK, 0.1 km from the industrial complex, October 1992-October 1993	0.22	43 (14-118)	
Flanders, Belgium 3 sites more than 10 km from the MWI, October – December 1993	-	8 (1.9-14)	*Fre et al*., 1994
Flanders, Belgium 5 urban and industrial sites, October – December 1993	-	76 (37-211)	
Flanders, Belgium 2 sites 0.6 km from the MWI, October – December 1993	-	567 (108-1025)	
UK, mean value for urban areas	0.31	48	*Duarte-Davidson et al*., 1997
UK, mean value for rural areas	0.35	12	
Germany, rural areas, 1993	0.3*	5-20	*Fiedler*, 1996
Germany, urban areas, 1993	0.3*	10-85	
Germany, close to point source, 1993	-	up to 1000	
Tartu, Estonia	-	1.6** (148)	*Brzuzy and Hites*, 1995
Rakvere, Estonia	-	0.4** (33)	
Saaremaa Island, Estonia	-	0.9** (82)	
Tallinn, Estonia, city center	-	1.0** 88	
Tallinn, Estonia, suburban	-	1.8** (159)	
Riga, Latvia	-	0.8** (74)	
Riga, Latvia	-	0.9** 77	
Vilnius, Lithuania	-	1.1** (96)	
Gorky park, Moscow, Russia	-	3.2** (293)	
Swan Lake, MT, USA	0.29	5.2** 469	
Yellowstone Lake, WY, USA	0.35	5.9** (532)	
Windermere Lake, Lake district, UK	0.30	30** (2713)	

* Ratio of the middle of deposition flux interval to that of typical air concentrations reported by *H.Fiedler* [1996].

** Calculated assuming that (pg/g soil)/(pg TEQ/g soil) = 90 (mean value of the ratio was calculated from data of *D.Broman et al*. [1990]); corresponding fluxes in pg/m^2 per day according to *L.P. Brzuzy and R.A. Hites* [1995] are given in brackets.

Flux values derived from soil and sediments concentrations are calculated as follows [*Brzuzy and Hites*, 1995; 1996]:

$$\text{Flux (pg/ m}^2\text{ yr)} = C/T, \qquad (3.1)$$

where C - density of soil pollution by PCDD/Fs, pg/ m^2;
T - time of accumulation, T = (Y - 1935) yr, where Y is the current year.

Derived soil and sediment fluxes are in a good agreement with each other and with some experimentally measured fluxes [*Brzuzy and Hites*, 1995], but it seems that this method gives underestimated values because it does not take into account PCDD/Fs degradation and volatilisation.

Estimation of PCDD/Fs deposition velocity using data on air concentrations and deposition fluxes gives some unexpected results. First, deposition velocity is almost the same in different sites (see Table 3.2). Second, no significant difference in deposition velocities for individual PCDD/F congeners has been found [*Jones and Duarte-Davidson*, 1997] in spite of differences in congeners physico-chemical properties and gas/particle distribution. Third, dry deposition velocity of aerosol particles of <1.35 μm in diameter, which contain more than 90% of atmospheric PCDD/Fs [*Kaupp et al*., 1994] is an order of magnitude lower than measured deposition velocities [*Jones and Duarte-Davidson*, 1997].

Effective washout ratio is calculated as a sum of washout ratios for gaseous and aerosol fractions:

$$W = W_v(1-\phi) + W_p\phi, \qquad (3.2)$$

where W_v and W_p - washout ratios for gaseous and aerosol fractions, equal to the ratio of the bulk concentration of each fraction in the precipitation to that in air;
ϕ - fraction of particulate pollutant in its total air concentration.

Washout ratio for gaseous fraction of organic pollutants is calculated as follows:

$$W_v = RT/H = 1/K_H \qquad (3.3)$$

where R - gas constant, Pa×m^3/mol.K;
T - temperature, ^{0}C;
H- Henry law constant, Pa×m^3/mol;
K_H – dimensionless Henry law constant, $K_H = H/RT$.

Table 3.3 summarises the measured W_v values for PCDD/Fs [*Eitzer and Hites*, 1989]

Table 3.3 Measured W_v values for PCDD/Fs [*Eitzer and Hites*, 1989]

PCDD/Fs	Measured W_v (5 – 30^{0}C)
TCDF	16 000
PeCDF	9 300
HxCDF	8 600
HpCDF	58 000
OCDF	210 000
PeCDD	6 300
HxCDD	5 600
HpCDD	270 000
OCDD	2 700 000

4. Parameters of PCDD/Fs migration and degradation in the environment

All found experimental data on PCDD/Fs physico-chemical properties had been obtained before 1990 and reviewed by *W.Shiu et al*. [1988] and *D.Mackay et al*. [1992]. Up to now these two compendia are the main sources of information for estimation of PCDD/Fs migration parameters (see, for example, *P.Ruelle and V.Kesselring* [1997], *W.Brubaker and R.Hites* [1997], *P.Chrostovski and S.Foster* [1986]). Experimental data exist only for a few PCDD/Fs congeners, and there is a considerable variation between reported values. For this reason it was proposed to estimate PCDD/Fs properties using simple correlation based on general physico-chemical consideration, empirical rules and all available experimental data [*Shiu et al*., 1988]. This approach was used by *B.Rordorf* [1989] for prediction of PCDD/Fs vapour pressure and in the present work for estimation of PCDD/Fs solubilities. Thus, this method allows to obtain the self-agreed sets of parameters for PCDD/Fs as a whole.

4.1 Melting and boiling points

Experimentally measured melting points and predicted boiling points of PCDD/Fs from *B.Rordorf* [1989] are given in Table 4.1.

Table 4.1 Melting and boiling points of PCDD/Fs

Chlorine positions	Melting point, ^{0}C (experimental)	Boiling point, ^{0}C (predicted)
Dibenzo-*p*-dioxins		
2,3,7,8	305-306	446.5
1,2,3,7,8	240-241	464.7
1,2,3,4,7,8	273-275	487.7
1,2,3,6,7,8	285-286	487.7
1,2,3,7,8,9	243-244	487.7
1,2,3,4,6,7,8	264-265	507.2
1,2,3,4,6,7,8,9	330-332	510
Dibenzofurans		
2,3,7,8	227-228	438.3
1,2,3,7,8	225-227	464.7
2,3,4,7,8	196-196.5	464.7
1,2,3,4,7,8	222.5-226.5	487.7
1,2,3,6,7,8	232-234	487.7
1,2,3,7,8,9	-	487.7
2,3,4,6,7,8	239-240	487.7
1,2,3,4,6,7,8	236-237	507.2
1,2,3,4,7,8,9	221-223	507.2
1,2,3,4,6,7,8,9	258-260	537

4.2 Solubility in water

The following data were used for the estimation of PCDD/Fs solubility in water at 25^{0}C: experimentally measured values; values selected from published experimental data; calculated values. The most recent experimentally measured values were selected as a rule from published data.

Solubility of PCCD/Fs in water as a function of temperature was estimated by the following equations: $\log S_m = \Delta H_{sol}/2.303RT + a,$ (4.1)

where S_m - solubility, mol/l;
$S_m(25^0C)$ - solubility at 25^{0}C, mol/l;
ΔH_{sol} - enthalpy of solubilization, J/mol;
T – temperature, K;
R - gas constant, R = 8.314 J/mol×K;
a – constant, $a = \log S_m(25^0C) - \Delta H_{sol}/2.303R\times298$.

Published and selected solubility values for PCDD/Fs are given in Table 4.2. Published values are given with indication of method of their determination and reference.

Table 4.2 Published and selected solubility values for PCDD/Fs solubility in water at 25^0C

Chlorine positions	Solubility at 25^0C , μmol/m^3 (10^{-9}mol/l)	Selected value
Dibenzo-*p*-dioxins		
2,3,7,8	0.06[a,2; c,2], 0.05[f,2], 0.16[c,3]	0.06
1,2,3,7,8		0.04
1,2,3,4,7,8	0.11 (20^0C) [a,2; c,2], 0.020 (26^0C)[b, 1] , 0.006[c,3]	0.02
1,2,3,6,7,8		0.02
1,2,3,7,8,9		0.02
1,2,3,4,6,7,8	0.0056 (20^0C) [a,2; c,2], 0.0060 (26^0C)[b,1], 0.0009 (20^0C) [c,3]	0.006
1,2,3,4,6,7,8,9	0.00016[a,1; c,2]	0.00016
Dibenzofurans		
2,3,7,8	1.4 [d,1,c,2], 1.7[c,3]	1.4
1,2,3,7,8		1.0
2,3,4,7,8	0.69 [d,1,c,2], 0.44[c,3]	0.69
1,2,3,4,7,8	0.022 [d,1,c,2], 0.026[c,3]	0.022
1,2,3,6,7,8	0.047 [d,1,c,2], 0.030[c,3]	0.047
1,2,3,7,8,9		0.04
2,3,4,6,7,8		0.04
1,2,3,4,6,7,8	0.0033 [d,1,c,2], 0.030[c,3]	0.0033
1,2,3,4,7,8,9		0.0033
1,2,3,4,6,7,8,9	0.0026 [e,1,c,2], 0.00031[c,3]	0.0026

For some PCDD/Fs the experimental data were not found. In these cases solubilities and enthalpies of solubilization were estimated using data for the nearest homologue. The following assumptions were made:

- solubilities and enthalpies of solubilization for PCDD/F homologue groups with the same chlorine number are approximately the same;
- solubility of PCDD/Fs decreases with the increase of chlorine number.
- enthalpy of solubilization for tetra-, penta-, hexa-, and hepta-PCDFs is close to enthalpies of solubilization for corresponding PCDDs and equal to 45 kJ/mol.

Estimated temperature dependencies are given in Table 4.3.

Table 4.3 Solubility of PCCD/Fs in water as a function of temperature

Chlorine positions	ΔH_{sol}, kJ/mol	Selected value of ΔH_{sol}, kJ/mol	Temperature dependence of log(S, mol/m^3)
Dibenzo-*p*-dioxins			
2,3,7,8	46.9 [e,1]*, 33.4 [a,1]*, 39.8 [b,1]**	40	-2089/T - 0.21
1,2,3,7,8	47.5 [b,1]***	47.5	-2481/T +0.93
1,2,3,4,7,8	45.5 [b,1]	45.5	-2376/T + 0.27
1,2,3,6,7,8		45.5	-2376/T + 0.27
1,2,3,7,8,9		45.5	-2376/T + 0.27
1,2,3,4,6,7,8	42.2 [b,1]	42.2	-2204/T - 0.82
1,2,3,4,6,7,8,9	74.5 [e,1]	74.5	-3891/T + 3.26
Dibenzofurans			
2,3,7,8		45	-2345/T + 2.01
1,2,3,7,8		45	-2345/T + 1.87
2,3,4,7,8		45	-2345/T + 1.71
1,2,3,4,7,8		45	-2345/T + 0.21
1,2,3,6,7,8		45	-2345/T + 0.54
1,2,3,7,8,9		45	-2345/T + 0.47
2,3,4,6,7,8		45	-2345/T + 0.47
1,2,3,4,6,7,8		45	-2345/T - 0.61
1,2,3,4,7,8,9		45	-2345/T - 0.61
1,2,3,4,6,7,8,9	62.6 [e,1]	62.6	-3269/T + 2.39

* - ΔH_{sol} for 1,2,3,4 -TCDD
** - ΔH_{sol} for 1,2,3,7 -TCDD
*** - ΔH_{sol} for 1,2,3,4,7 -PeCDD

References:
a – [*Shiu et al*., 1988]
b – [*Friesen and Webster*, 1990]
c – [*Ruelle and Kesselring*, 1997]
d – [*Friesen et al*., 1990b]
e – [*Doucette and Andern*, 1988]
f – [*Schwarzenbach et al.,* 1993]

4.3 Vapour pressure

Based on experimentally measured vapour pressure for 10 PCDDs, *B.Rordorf* [1989] estimated vapour pressures for most PCDD/Fs. Boiling points, enthalpies and entropies of evaporation, sublimation and fusion were also predicted. Temperature dependencies of PCDD/Fs vapour pressure derived from these estimates are given in Table 4.4.

Table 4.4 Temperature dependence of vapour pressure of PCCD/Fs

Chlorine Positions	Temperature dependence of vapour pressure	
	$\log(p_S, Pa)$	$\log(p_L, Pa)$
Dibenzo-*p*-dioxins		
2,3,7,8	-6477/T + 15.02	-4392/T + 11.42
1,2,3,7,8	-7003/T + 16.25	-4778/T + 11.90
1,2,3,4,7,8	-7354/T + 16.35	-4840/T + 11.75
1,2,3,6,7,8	-7312/T + 16,19	-4803/T + 11.41
1,2,3,7,8,9	-7466/T + 16.87	-4957/T + 12.01
1,2,3,4,6,7,8	-7825/T + 17.13	-5017/T+ 11.91
1,2,3,4,6,7,8,9	-7895/T + 16.53	-4676/T+ 11.20
Dibenzofurans		
2,3,7,8	-6253/T + 15.25	-4344/T + 11.46
1,2,3,7,8	-6737/T + 15.98	-4504/T + 11.54
2,3,4,7,8	-6813/T +16,40	-4607/T + 11.70
1,2,3,4,7,8	-7177/T + 16.56	-4655/T + 11.54
1,2,3,6,7,8	-7161/T + 16.45	-4645/T + 11.49
1,2,3,7,8,9*	-7161/T + 16.47	-4643/T + 11.51
2,3,4,6,7,8	-7146/T +16.40	-4629/T + 11.49
1,2,3,4,6,7,8	-7556/T + 17.03	-4735/T + 11.49
1,2,3,4,7,8,9	-7586/T + 17.23	-4777/T+ 11.43
1,2,3,4,6,7,8,9	-7806/T + 16.88	-4805/T + 11.24

* Coefficients of temperature dependence for 1,2,3,7,8,9-HxCDF are assumed to be equal to average values of corresponding coefficients for other HxCDF

The solid vapour pressure temperature dependencies (p_S, Pa) were obtained by the following equation:

$$p_S = \exp[(\Delta S_s T - \Delta H_s)/RT], \quad (4.2)$$

where R - gas constant (8.314 J/mol×K);
ΔS_s and ΔH_s - entropy(J/mol×K) and enthalpy (J/mol) of sublimation correspondingly;
T - temperature (K).

The subcooled liquid vapour pressure temperature dependences (p_L , Pa) were estimated as:

$$p_L = p_S \times \exp[\Delta S_f(T_m/T - 1)/R], \quad (4.3)$$

where ΔS_f - entropy of fusion(J/mol×K);
T_m - melting point (K).

4.4 Henry law constant

Temperature dependencies of Henry law constant for PCDD/Fs are given in Table 4.5. They were calculated using the following equation:

$$\log H = \log p_S - \log S_m \quad (4.4)$$

Table 4.5 Temperature dependencies of Henry law constant for PCDD/Fs

Chlorine positions	Temperature dependence of Henry law constant Log(H, Pa×m^3/mol)
Dibenzo-*p*-dioxins	
2,3,7,8	-4388/T + 15.02
1,2,3,7,8	-4522/T + 15.32
1,2,3,4,7,8	-4978/T + 16.08
1,2,3,6,7,8	-4936/T + 15.92
1,2,3,7,8,9	-5090/T + 16.60
1,2,3,4,6,7,8	-5621/T + 17.95
1,2,3,4,6,7,8,9	-4004/T +13.27
Dibenzofurans	
2,3,7,8	-3908/T + 13.24
1,2,3,7,8	-4392/T + 14.11
2,3,4,7,8	-4468/T + 14.69
1,2,3,4,7,8	-4832/T + 16.35
1,2,3,6,7,8	-4816/T + 15.91
1,2,3,7,8,9*	-4816/T + 16.00
2,3,4,6,7,8	-4801/T + 15.93
1,2,3,4,6,7,8	-5211/T + 16.42
1,2,3,4,7,8,9	-5241/T + 16.62
1,2,3,4,6,7,8,9	-4537/T + 14.59

* Coefficients of temperature dependence for 1,2,3,7,8,9-HxCDF were assumed to be equal to average values of corresponding coefficients for other HxCDF.

Table 4.6 presents the calculated PCDD/Fs Henry law constants summarised by *D. Mackay et al.* [1992]:

Table 4.6 Calculated PCDD/Fs Henry law constants [*Mackay et al., 1992*]

Henry law constant, Pa m^3/mol			
PCDD		PCDF	
2378TCDD	0.0021 [*Mabey et. al*., 1982]	2378TCDF	1.50 [*Eitzer & Hites*, 1989]
	0.152 [*Crosby*, 1985]		
	0.212 [*Schroy et. al*., 1985]		
	1.64 [*Podoll et. al*., 1986]		
	1.63; 3.34; 10.34 [*Shiu et. al*., 1985, 1988]		
	7.93 [*Jury et. al*., 1990]		
12347PeCDD	0.264 [*Shiu et. al*, 1988]		
123478HxCDD	4.52 [*Shiu et. al*, 1988]		
1234678HpCDD	0.133 [*Shiu et. al*, 1988]		
OCDD	0.683 [*Shiu et. al*, 1987, 1988]	OCDF	0.10 [*Clark & Mackay*, 1991]

4.5 Partition coefficients in soil and bottom sediments

PCDD/Fs partition coefficient in soils and bottom sediments can be calculated as follows:

$$K_p = K_{oc} f_{oc} \quad (4.5)$$

where K_p - partition coefficient, l/kg;
K_{oc} - organic carbon-water partitioning coefficient, l/kg;
f_{oc} - organic carbon fraction in soil or sediments (kg/kg dry weight).

K_{oc} is usually estimated by correlation with octanol-water partition coefficient (K_{ow}). For example, equation $K_{oc} = 0.41K_{ow}$, obtained by *S.Karikhoff et al*. [1979], was used for the calculation of K_p for 2,3,7,8-TCDD [*Vozhzennikov et al.*, 1997]. Values of $\log K_{ow}$ for PCDD/Fs from *D.Mackay et al*. [1992] are given in Table 4.7.

Table 4.7 Octanol-water partition coefficients for PCDD/Fs (from [*Mackay et al.*, 1992])

PCDD/F	$\log K_{ow}$
TCDD	6.8
PeCDD	7.4
HxCDD	7.8
HpCDD	8.0
OCDD	8.2
TCDF	6.1
PeCDF	6.5
HxCDF	7.0
HpCDF	7.4
OCDF	8.0

4.6 PCDD/Fs gas-aerosol partition

Organic pollutant distribution between aerosol particles and air is quantitavely characterised by partition coefficient K_{pa}, which is equal to the ratio of pollutant amount retained by filter to that retained by absorber:

$$K_{pa} = F/A \text{ (TSP)}, \quad (4.6)$$

where F - air concentration of PCDD/Fs retained by filter, ng/m^3;
A - air concentration of PCDD/Fs retained by absorber, ng/m^3;
TSP - content of aerosol particles in air, μg/m^3.

Dependence of K_{pa} on ambient temperature is usually described by the following equation:

$$\log K_{pa} = m_p/T + b_p \quad (4.7)$$

where m_p and b_p - constants for an individual compound.
Equation connecting partition coefficient and vapour pressure of subcooled liquid is also used:

$$\log K_{pa} = m_r \log p_L + b_r, \quad (4.8)$$

where m_r and b_r - constants for a class of compounds.

Existing experimental data do not allow us to obtain statistically significant estimation of coefficients used in equation 4.7 for each PCDD/F. More data are available for the estimation of K_{pa} temperature dependence for PCDD/Fs as a class of compounds in the form of equation 4.8. We obtained such a dependence with the least square method using experimentally measured aerosol/gas distribution of 7 PCDFs and 3 PCDDs at 8 different temperature values in the range of 0-20^{0}C [*Hippelein et al.*, 1996] and temperature dependencies of subcooled liquid vapour pressures given in Table 4.4 (36 $\log K_{pa}$-$\log p_L$ pairs). The correlation equation is given bellow:

$$\log K_{pa} = -1.24 \log p_L - 6.70, \quad R^2 = 0.94 \qquad (4.9)$$

Figure 4.1 is the plot of regression line and experimental data. It can be seen that in all cases the discrepancies of calculated and experimental values are smaller than 0.5 log unit, that means that K_{pa} and p_L are correlated with an accuracy within a factor of 3 or better.

Such accuracy is believed to be sufficiently reliable for environmental modelling. The temperature dependence of K_{pa} for an individual PCDD/F can be obtained from equation 4.9 by substitution of $\log p_L$ with corresponding data from table 4.4.

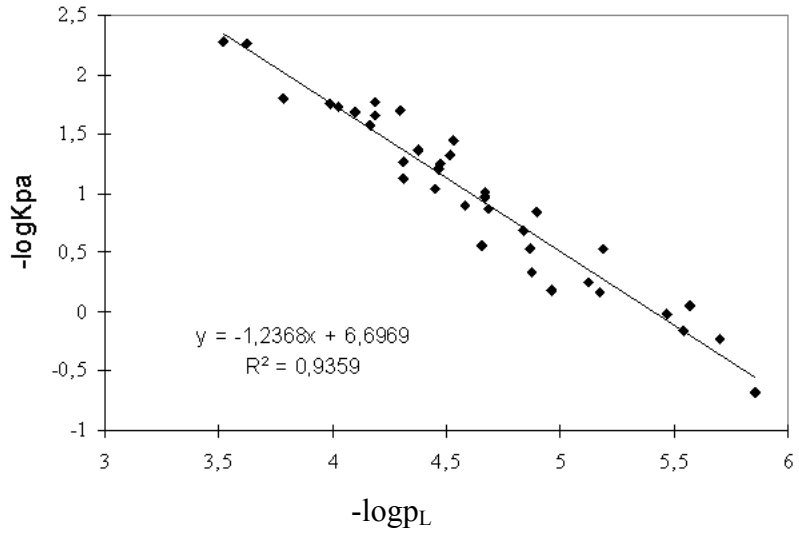

Figure 4.1 Dependence of $\log K_{pa}$ on $\log p_L$ for PCDD/Fs

The percentage of particulate fraction for 2,3,7,8-chlorine substituted congeners was estimated on the basis of equations 4.6 and 4.9 at –10^{0}C and +20^{0}C assuming that TSP is equal to 50 μg/m^3. Results are summarized in table 4.8.

Table 4.8 Percentage of particulate fraction for 2,3,7,8-chlorine substituted congeners at –10^{0}C and +20^{0}C

Homologue group	% of particulate fraction	
	–10^{0}C	+20^{0}C
TCDD	97	21

PeCDD	>99	74
HxCDD	>99	92
HpCDD	>99	97
OCDD	>99	89
TCDF	95	13
PeCDF	>99	36
HxCDF	>99	71
HpCDF	>98	89
OCDF	>99	96

Thus, contribution of gas fraction is significant only for TCDD/Fs and PeCDF in summer time.

4.7 PCDD/Fs degradation in the environment

4.7.1 Degradation in the atmosphere

Organic chemicals degrade in the atmosphere due to direct photolysis and reactions with photochemically generated oxidants (O_3, $NO_3^{\bullet}$, $OH^{\bullet}$ etc.). According to *E.Kwok et al*. [1994, 1995] and *W.Brubaker et al*. [1997] the main mechanism of PCDD/Fs degradation in the troposphere is a reaction with hydroxyl-radical, other processes can be neglected. The first order rate constant of PCDD/Fs degradation in respect to the reaction with hydroxyl-radical can be calculated as follows:

$$k^*_{OH} = k_{OH}[OH], \qquad (4.10)$$

where k^*_{OH} - the first order rate constant, s^{-1};
k_{OH} - the second order rate constant, $cm^3 \times molecule^{-1} \times s^{-1}$;
[OH] - hydroxyl-radical concentration, molecules/cm^3.

In 45^0N daily average $OH^{\bullet}$ concentration in overground air layer of 2 km height is 2×10^6 molecules/cm^3 in summer, 0.8×10^6 molecules/cm^3 in the fall/spring, and 0.09×10^6 molecules/cm^3 in winter [*Yu Lu and Khall*, 1991]. Seasonally averaged values of k^*_{OH}, calculated using these data and the second order rate constant predicted by *R.Atkinson* [1996] are given in Table 4.9.

Table 4.9 Values of k^*_{OH} for PCDD/Fs

PCDD/Fs	$k_{OH}\times10^{-12}$ $cm^3\times molecule^{-1}\times s^{-1}$ [*Atkinson*, 1996]	k^*_{OH}, d^{-1}			
		Summer	fall/spring	winter	yearly averaged
TCDD	1.05	0.18	0.073	0.0082	0.088
PeCDD	0.56	0.097	0.039	0.0043	0.047
HxCDD	0.27	0.047	0.042	0.0021	0.022
HpCDD	0.13	0.022	0.0086	0.0010	0.011
OCDD	0.05	0.009	0.003	0.0004	0.04
TCDF	0.61	0.11	0.042	0.0047	0.052
PeCDF	0.30	0.052	0.021	0.0023	0.025
HxCDF	0.14	0.024	0.0095	0.0011	0.012
HpCDF	0.06	0.01	0.004	0.0004	0.005
OCDF	0.03	0.005	0.002	0.0003	0.003

Taking into account the fact that the photodegradation of particle-bound PCDD/Fs was found to be negligible [*Koester and Hites*, 1992], the effective rate constant k_{ef} for degradation of both particulate and gaseous fractions of these compounds in the atmosphere can be calculated as follows:

$$k_{ef} = \phi_v k^*_{OH}, \qquad (4.11)$$

where ϕ_v - fraction of gaseous PCDD/Fs calculated from K_{pa} and TSP.

4.7.2 Degradation in natural waters

Main pathways of organic chemical degradation in natural waters are hydrolysis, photolysis and biodegradation. As it was shown by *K.Friesen et al*. [1990a], indirect photolysis synthesized by dissolved organic matter (DOM) is the prevailing mechanism of PCDD/F degradation in pond water. This process can occur via energy transfer from DOM to PCDD/Fs or via PCDD/Fs reactions with oxidants generated as a result of sunlight absorption by DOM. The most important photogenerated oxidant responsible for organic pollutants scavenging in natural waters is hydroxyl radical. The effective rate constant of pollutant reaction with hydroxyl radical can be estimated as:

$$k^{*w}_{OH} = k^w_{OH}[OH], \qquad (4.12)$$

where k^{*w}_{OH} - the first order rate constant, s^{-1};
k^w_{OH} - the second order rate constant, $l\times mol^{-1}\times s^{-1}$;
[OH] - hydroxyl-radical concentration, mol/l.

Yearly averaged concentrations of hydroxyl radicals in natural surface waters are given in Table 4.10.

Table 4.10 Yearly averaged concentrations of hydroxyl-radicals in natural surface waters

Type of surface natural water	$OH^{\bullet}$ concentration, mol/l	References
Rivers and fresh water lakes	2×10^{-16}	*L. Ernestova and I.Semenova,* 1995a, 1995b *Yu.Skurlatov et al*. 1994 *E.Shtamm et al*. 1991
Coastal see water	10^{-17}	*K.Mooper et al*. 1990
Ocean	5×10^{-19}	*K.Mooper et al*. 1990 *E.Shtamm et al*. 1991

Using hydroxyl radical concentrations from Table 4.8 and $k^{w}_{OH} = 4\times10^{9}$ $l\times mol^{-1}\times s^{-1}$ estimated by *W.G.Haag and C.C.D.Yao* [1992], we calculated the effective rate constants for 2,3,7,8-TCDD reaction with hydroxyl radical in natural waters. In rivers and fresh water lakes k^{*}_{OH} is equal to 0.07 d^{-1}, in coastal sea waters - 0.003 d^{-1}, in open ocean - 0.0002 d^{-1}. The calculated k^{*}_{OH} value for fresh waters is about an order of magnitude smaller than rate constants of 0.74 and 0.28 d^{-1} measured for 1,2,3,4,7-PeCDD and 1,2,3,4,6,7,8-HpCDD photolysis in pond water under midsummer sunlight conditions at 50^{0}N latitude [*Friesen et al*., 1990a]. This discrepancy can be explained by higher hydroxyl radical concentration in conditions of the experiment in comparison with the yearly averaged concentration used in calculations. The main mechanism of hydroxyl radical formation is photochemical reaction, its rate depends on sunlight intensity. The most photochemically active ultraviolet part of sunlight is several times more intensive in midsummer than in the rest of the year [*Leifer*, 1988]. In addition, DOM content in pond water in the experiment was about 3-6 times higher than average DOM content in natural fresh waters, that should result in corresponding increase of photosynthesized degradation rate of organic pollutants [*Sychev et al*., 1983]. Thus, calculated values of rate constants for 2,3,7,8-TCDD reaction with hydroxyl radical are quite realistic and can be used for the estimation of PCDD/F degradation rates in natural waters.

Rate constants of 0.058 and 0.019 d^{-1} were measured for direct photolysis of 1,2,3,4,7-PeCDD and 1,2,3,4,6,7,8-HpCDD under midsummer sunlight conditions at 50^{0}N latitude in distilled water-acetonitrile (2:3 v/v) solution [*Friesen et al*., 1990a]. It means that direct photolysis contributes significantly to PCDD/Fs degradation, especially in seawaters. The direct photolysis rate of organic pollutants in water can be calculated from the spectrum of solar radiation, absorption spectrum and quantum yield of pollutant photodegradation. Unfortunately, absorption spectrum and quantum yield for PCDD/Fs can be measured only in water-cosolvent solutions. Uncertainties of such measurements are very high. That is why it seems to be reasonable to use rate constants measured by *K.Friesen et al*. [1990], taking into account that yearly average direct photolysis rate constant for PCDD/Fs is about 2,5 times smaller than it is in midsummer [*Podoll et al*., 1986].

Based on the above consideration we estimated the effective rate constants of PCDD/Fs degradation in natural waters. The following assumptions were made:

- k^{w}_{OH} for tetra-, penta- and hexachloro-DD/Fs is the same as for 2,3,7,8-TCDD and equal to 4×10^{9} $l\times mol^{-1}\times s^{-1}$;

- k^{w}_{OH} for hepta- and octachloro-DD/Fs is equal to 2×10^{9} $l\times mol^{-1}\times s^{-1}$;
- yearly average rate constant of direct photolysis for tetra-, penta- and hexachloro-DD/Fs is the same as for 1,2,3,4,7-PeCDD and equals to $0.058 : 2.5 \approx 0.02$ d^{-1};
- yearly average rate constant of direct photolysis for hepta- and octachloro-DD/Fs is the same as for 1,2,3,4,6,7,8-HpCDD and equals to $0.019 : 2.5 \approx 0.01$ d^{-1}.

Estimated effective rate constants of PCDD/Fs degradation in natural waters are given in Table 4.11.

Table 4.11 Rate constants of PCDD/Fs degradation in natural waters due to reaction with hydroxyl-radicals and direct photolysis

PCDD/F	k^{*w}_{OH}, d^{-1}		
	rivers and fresh water lakes	coastal sea waters	open ocean
TCDD	0.09	0.02	0.02
PeCDD	0.09	0.02	0.02
HxCDD	0.09	0.02	0.02
HpCDD	0.05	0.01	0.01
OCDD	0.05	0.01	0.01
TCDF	0.09	0.02	0.02
PeCDF	0.09	0.02	0.02
HxCDF	0.09	0.02	0.02
HpCDF	0.05	0.01	0.01
OCDF	0.05	0.01	0.01

The half-lives of PCCD/Fs in the Baltic Sea sediments calculated from their vertical profiles range from 29 to 79 years for PCDFs and from 102 to 173 years for PCDDs [*Kjeller and Rappe*, 1994].

4.7.3 Degradation in soil

Measurement of PCDD/Fs degradation rate constant in soil is a difficult task due to their stability to microbiological degradation. However, there are a few data about PCDD/Fs degradation half-lives in soils. Mean 2,3,7,8-TCDD half-life in soil around Seveso (Milan, Italy) was equal to 9.1 years [*Cerlesi et al*., 1989]. Therefore it can be assumed that average PCDD/Fs degradation half-life in Europe is not less than 10 years.

5. Conclusions

Analysis of available data on PCDD/PCDF physico-chemical properties and their fate in the environment has shown that:

- There are 10 PCDD/F homologue groups of environmental interest. Each of them could be regarded as a single substance. More detailed consideration is impossible due to the lack of data on congener-specific physico-chemical properties.

- A few experimentally measured physico-chemical data reliable for estimation of PCDD/F migration parameters is available at present;
- There is a considerable variation between published values of the same parameter;
- Rate constants of PCDD/F degradation in the atmosphere, natural waters and soils can be estimated only with accuracy of an order of magnitude;
- Data on emission factors and relative contributions of the main PCDD/F emission source categories to the total emission are available only for some European countries;
- Homologue pattern of atmospheric PCDD/Fs can be estimated with appropriate accuracy;
- Homologue patterns of atmospheric PCDD/Fs in urban areas are quite similar, and since urban areas are the main source of PCDD/F emissions one can estimate the percentage of homologue groups in the total emission;
- Contribution of PeCDD/Fs and HxCDD/Fs to the total atmospheric concentration in pg TEQ/m^3 in urban area is more than 80% while the contribution of other homologue groups is less than 20%;
- No significant difference in deposition velocities for individual PCDD/PCDF congeners were found in spite of the differences in their physico-chemical properties, gas/aerosol partitioning and site of sampling;
- Chlorine number in the PCDD/F molecule has a significant effect on its physico-chemical properties;
- Simple correlation and empirical rules should be used for the estimation of PCDD/F physico-chemical properties and degradation rates;
- All PCDD/F homologue groups excepting TCDD/Fs and PeCDF occur in aerosol fraction within the whole year. Contribution of gas fraction is significant only for TCDD/Fs and PeCDF in summer time;
- The exchange processes between the atmosphere and soil, water as well as vegetation require the more detailed study and analysis.

Taking into account the above conclusions, the following approach in PCDD/PCDFs modelling can be proposed as the first stage. PCDD/Fs are divided into two groups according to their physico-chemical properties, gas/aerosol partitioning, degradation rate in the atmosphere and contribution to the total atmospheric concentration:

- TCDD/Fs and PeCDF which occur in the air in summer time mainly in the gaseous form and have the effective degradation half-lives in the atmosphere about 10 days. PeCDF contribute about 80% to the atmospheric concentration (in pg TEQ/m^3) of this group. Therefore it seems reasonable to use the PeCDF migration parameters for modelling of the airborne transport of this group;
- Other PCDD/Fs which are almost completely associated with aerosol particles and have degradation half-lives in the atmosphere from several months to several years. Migration parameters for modelling of this group are under investigation.

References

Atkinson R. [1996] In: Issues in Environmental Science and Technology. Hester R.E., Harrison R.M. (Eds.) The Royal Society of Chemistry, Cambridge, U.K., v. 6, pp. 53-72.

Atmospheric Emission Inventory Guidebook [1996]. EMEP/CORINAIR, Copenhagen.

Berdowski, J.J.M., J. Baas , J.P.J. Bloos, A.J.H. Visschedijk and P.Y.J. Zandveld [1997] The European Emission Inventory of Heavy Metals and Persistent Organic Pollutants for 1990. TNO Institute of Environmental Sciences, Energy Research and Process Innovation, UBA-FB report 104 02 672/03, Apeldoorn, p. 239.

Bosworth WS, Thibodeaux LJ. Bioturbation [1990] A Facilitator of Contaminant Transport in Bed Sediment. Env Prog, v. 9, № 4, pp. 211-217.

Broman D., Naf C., Rolf C., Zebuhr Y. [1990] Analysis of polychlorinated dibenzo-p-dioxins (PCDD) and polychlorinated dibenzofurans (PCDF) in soils and digested sewage from Stockholm, Sweden. Chemosphere, v. 21, № 10-11, pp. 1213-1220.

Brubaker WW, Hites RA. [1997] Polychlorinated dibenzo-p-dioxins and dibenzofurans: gas-phase hydroxyl radical reactions and related atmospheric removal. Environ Sci Technol, v.31, № 6, pp. 1805-1810.

Brzuzy LP, Hites RA. [1995] Estimating the atmospheric deposition of polychlorinated dibenzo-p-dioxins and dibenzofurans from soils. Environ Sci Technol, v.29, № 8, pp. 2090-2098.

Brzuzy LP, Hites RA. [1996] Clobal mass balance for polychlorinated dibenzo-p-dioxins and dibenzofurans. Environ Sci Technol, v. 30, № 6, pp.1797-1804.

Bulgakov AA, Konoplev AV, Shkuratova IG. [1997] Empiric time dependence of radiocesium fraction in the upper layer of soil in the Chernobyl zone. Pochvovedenie ; submitted.

Bulgakov, A.A., Konoplev, A.V., Popov, V.E., Bobovnikova, T.I., and Shkuratova, I.G. [1992] Mechanisms of long-lived radionuclides migration in soils of 30-km Chernobyl NPP zone. Pochvovedenie № 11, pp.14-19.

Cerlesi S, di Domenico A, Ratti S. [1989] 2,3,7,8-Tetrachlorodibenzo-p-dioxin (TCDD) persistence in the Seveco (Milan, Italy) soil. Ecotoxicology and Environmental Safety; v. 18 pp.149-164.

Chrostowski PC, Foster SA. (1986) A methodology for assessing congener-specific partitioning and plant uptake of dioxins and dioxin-like compound. Chemosphere; 32: 11.2285-2304.

Clark K.E., Mackay D. [1991] Dietary uptake and biomagnification of four chlorinated hydrocarbons by guppies. Environ.Toxicol.Chem., v.37, pp.251-254.

Creaser CS, Fernandes AR, Harrad SJ, Cox EA. [1990] Levels and sources of PCDDs and PCDFs in urban British soils. Chemosphere, v.21, № 8, pp.931-938.

Crosby D.G. [1985] The degradation and disposal of chlorinated dioxins. In: Dioxins in the Environment. Kamrin M.A., Rogers P.W., Editors, Hemisphere Publication Corporation, Washington, pp.195-204.

Doucette WJ, Andren AW. [1988] Aqueous solubility of selected biphenyl, furan, and dioxin congeners. Chemosphere, v.17, №2, pp.243-252.

Douben P.E.T. [1997]. PCDD/F emissions to atmosphere in the UK and future trends. Chemosphere, v.34, №5-7, pp.1181-1189.

Duarte-Davidson R, Sewart A, Alcock RE, Cousins IT, Jones KC. [1997] Exploring the balance between sources, deposition and the environmental burden of PCDD/Fs in the U.K. terrestrial environment: an aid to identifying uncertainties and research needs. Environ. Sci. Technol, v.31, №1,pp.1-11.

Eitzer BD, Hites RA. [1989] Atmospheric transport and deposition of polychlorinated dibenzo-p-dioxins and dibenzofurans. . Environ. Sci. Technol, v.23, №11, pp.1396-1401.

Ernestova L.S., Semenova I.V. [1995a] Distribution particularities of hydroxyl radicals in the lakes ecological systems. Meteorologiya and Gidrologiya, №8, pp. 101-110. (in Russian)

Ernestova L.S., Semenova I.V. [1995b] Anthropogenic influence on hydroxyl radicals content in the large rivers. Meteorologiya and Gidrologiya, №6, pp.95-106. (in Russian).

Fre R.De., Wevers M., Van Cleuvenbergen R., Schoeters J. [1994] Measurement of dioxins in Flanders, Belgium. Organoclorine Compounds, v. 20, pp.9-14.

Fiedler H. [1996] Sources of PCDD/PCDF and impact on the environment. Chemosphere; v.32, №1, pp.55-64.

Friesen K.J, Muir D.C.G, Webster G.R.B. [1990a] Evidence of sensitized photolysis of polychlorinated dibenzo-p-dioxins in natural waters under sunlight conditions. Environ. Sci. Technol., v.24, № 11, pp.1739-1744.

Friesen K.J., Vilk, J. and Muir D.C.G. [1990b] Aqueous solubilities of selected 2,3,7,8-substituted polychlorinated dibenzofurans (PCDFs). Chemosphere v.20, № 1-2, pp.27-32.

Friesen K.J. and Webster G.R.B. [1990] Temperature dependence of the aqueous solubilities of highly chlorinated dibenzo-p-dioxins. Environ.Sci.Technol, v.24, № 1, pp.97-101.

Haag W.G., Yao C.C.D. [1992] Rate constants for reaction of hydrocyl radicals with several drinking water contaminants. Environmental Science and Technology, v.26, pp.1005-1-13.

Hagenmaier H, Lindig C., She J. [1993] Correlation of environmental occurence of polychlorinated dibenzo-p-dioxins and dibenzofurans with possible sources. Organohalogen Compounds, v.12, pp.271-274.

Hauk H. Umiauf G. McLachlan M.S. [1994] Uptake of gaseous DDE in spruce needles. Environmental Science and Technololy, v.28, pp.2372-2379.

Hippelein M, Kaupp H, Dorr G, McLachlan ML, Hutzinger O. [1996] Baseline contamination assessment for a new resources recovery facility in Germany. Part II: atmospheric concentrations of PCDD/F. Chemosphere, v.32, №8, pp.1605-1616.

Holoubec, I., J. Caslavsky, L. Nondek, A. Kocan, B. Pokorny, J. Lenicek, J. Hajslova, V. Kocourec, M. Matousek, J. Pacyna and D.J. Thomas [1993]. Compilation of Emission Factors for Persistent Organic Pollutants: A Case Study of Emission Estimates in the Czech and Slovak Republics. Masaryk University, Brno, Czech Republic and Axys Environmental Consulting Ltd. For External Affairs Canada, Ottawa. xii + 176 pp. + Appendix.

International toxicity equivalency factor (I-TEF) method of risk assessment for complex mixtures of dioxins and related compounds. [1988], p.176.

Jones K.C. [1997] Duarte-Davidson R. Transfer of airborne PCDD/Fs to bulk deposition collectors and herbage. Environ Sci Technol, v.31, №10, pp.2937-2943.

Jury W.A., Russo D., Streile G., El Abd H. [1990] Evaluation of volatilization by organic chemical residing below the soil surface. Water Resources Res., v.26, pp.13-26.

Karickhoff S.W. [1979] Brown DS, Scott TA. Sorption of hydrophobic pollutants on natural sediments. Water Res, v.13, pp.241-248.

Kaupp H, Towara J, McLachlan M.S. [1994] Distribution of polychlorinated dibenzo-p-dioxins and dibenzofurans in atmospheric particulate matter with respect to particle size. Atmospheric Environment, v.28, № 4, pp.585-593.

Kjeller L.-O., Rappe C. [1994] PCDD and PCDF in sediment core from the Baltic proper. Organoclorine Compounds, v.20, pp.115-120.

Koester CJ, Hites R.A. [1992] Photodegradation of polychlorinated dioxins and dibenzofurans adsorbed to fly ash. Environ. Sci. Technol., v.26, pp.502-507.

Konig J, Theisen J, Gunther W.J., Liebl K.H., Buchen M. [1993] Ambient air levels of polychlorinated dibenzofurans and dibenzo-p-dioxins at different sitesin Hessen. Chemosphere, v.26, pp.851-861.

Kwok E.S.C., Arey J, Atkinson R. [1994] Gas-phase atmospheric chemistry of dibenzo-p-dioxines and dibenzo-p-furanes. Environ. Sci. Technol., v.28, №3, pp.528-533.

Kwok E.S.C., Atkinson R, Arey J. [1995] Rate constants for the gas-phase reactions of the OH radical with dichlorobiphenyls, 1-chlorodibenzo-p-dioxin, 1,2-dimethoxybenzene, and diphenyl ether: estimation of OH radical reaction rate constants for PCBs, PCDDs, and PCDFs. Environ. Sci. Technol., v.29, №6, pp.1591-1598.

Leifer A. [1988] The kinetics of environmental aquatic photochemisty: theory and practice; American Chemical Society: Washington, p.262.

Lorber M., Cleverly D., Shaum J., Philips L., Schweer G., Lieghton T. [1994] Development and Validation of an air-to-beef food chain model for dioxin-like compounds. Organochlorine Compounds, 1994, v. 20, pp. 61-67.

Mabey W., Smith J.H., Podoll R.T., Johnson H.L., Mill T., Chou T.W., Gates J., Waight-Parridge I., Vanderberg D. [1982] Aquatic Fate Process for Organic Priority Pollutants. EPA Report No.440/4-81-014.

Mackay D., Shiu W.Y., Ma K.C. [1992] Illustrated handbook of physical-chemical properties and environmental fate for organic chemicals. (CRC. Press. Boca Raton, FL. 1992).

Matisoff G. [1982] Mathematical models of bioturbation. in McCall, P.L. and Tevesz, J.J.S. (eds): Animal-sedimant relations. NY, Plenum Press, pp 289-330.

Matsuda M., Horii Y., Seike N., Wakimoto T. [1997] The sampling and analysis of PCDD/Fs in water sample by means of co-precipitation. Organoclorine Compounds, v.31, pp.41-44.

Mooper K., Zhou Z. In: Blaugh N. V., Zepp R.G.(Eds) [1990] Effect of solar ultraviolet radiation on biogeochemical dynamics in aquatic environment. Woods Hole; Oceanografic Inst., p.151.(Citation from Schtamm et al. 1991).

Parma Z., Vosta J., Horejs J., Pacyna J.M. and Thomas D. [1995]. Atmospheric Emission Inventory Guidelines for Persistent Organic Pollutants (POPs). Prague, p.107.

Podoll R.T., Jaber H.M., Mill T. [1986] Tetrachlorodibenzodioxin: rates of volatilization and photolysis in the environment. Environmental Science and Technology, v.20, pp.490-292.

Rordorf B.F. [1989] Prediction of vapour pressure, boiling points and enthalpies of fussion for twenty-nine halogenated dibenzo-p-dioxins and fifty five dibenzofurans by a vapour pressure correlation method. Chemosphere, v.18, pp.783-788.

Ruelle P., Kesselring V.W. [1997] Aqueous solubility prediction of environmentally important chemical from the mobile order thermodynamics. Chemosphere, v.34, №2, pp.275-298.

Schroy J.M., Hileman F.D., Cheng S.C. [1985] Physical/chemical properties of 2,3,7,8-TCDD. Chemosphere, v.14, pp.873-886.

Schwarzenbach R.P., Gschwend P.M., Imboden D.M. [1993] Environmental organic chemistry. (Jonh Wiley & Sonc, Inc. New York 1993).

Shiu W.Y., Doucette W., Gobas F.A.P.C, Andren A., Mackay D. [1988] Physical-chemical properties of chlorinated dibenzo-p-dioxins. Environ. Sci. Technol., v.22, №6, pp.651-658.

Shtamm E.V., Purmal A.P., Skurlatov Yu.I. [1991] The role of hydrogen peroxide in the nature environment. Uspekhi Khimii, v.60, issue 11, pp.2373-2411.

Skurlatov Yu.I., Duka G.G., Mizity A. [1994] Introduction to the ecological chemistry. M.: Visshaya Shkola. (In Russian)

Sychev A.Ya., Travin S.O., Duka G.G., Scurlatov Yu.I. [1983] Catalitic reactions and environment protection. Kishenev (In Russian).

Thomas, V. and Spiro, T. [1996] The U.S. dioxin inventory: are there missing sources? Environ. Sci. Technol., v.30, №2, pp.82A-85A.

Tiernan T.O., Wagel D.J., VanNess G.F., Garrett J.H., Solch J.G., Harden L.A. [1989] PCDD/PCDF in the ambient air of a metropolitan area in the U.S. Chemosphere, v.19, № 1-6, pp.541-546.

Vozhzennikov O.I., Bulgakov A.A., Popov V.E. et al. [1997] Review of migration and transformation parameters of selected POPs, EMEP/MSC-E Report 3/97.

Wania F., Mackay D. [1996] Tracking the distribution of persistent organic pollutants. Environ. Sci. Technol., v.30, №9, pp.390A-396A.

Yufit S.S., Klyuev N.A. [1997] Analytical review of physical-chemical processes responsible for persistent xenobiotics input to and removal from the atmosphere of, Moscow, (in Russian).

Yu Lu and Khall M.A.K. [1991] Tropospheric OH: model calculation of spacial, temporal and secular variations. Chemosphere, v.23, pp.397-444.

APPENDIX A

Table A1 PCDD/Fs concentrations in the atmosphere, pg TEQ/m^3

Site	Sampling period	Concentration, pg TEQ/m^3	Reference
Dayton, Ohio, USA, Municipal waste incinerator (MWI) area	Spring 1988	≈ 0.4* (23 pg/m^3)	*Tiernan et al*., 1989
Germany, close to point source	1993, season is not specified	0.350-1.6	*Fiedler*, 1996
Hamburg, Germany, motorway tunnel	January 1986	≈0.5* (32 pg/m^3)	*Rappe et al*., 1988
Ufa, Russia, urban	1993, season is not specified	0.2-0.5	*Vozhzennikov et al.*, 1997
Bloomington, Indiana, USA, urban	1986 season is not specified	≈ 0.03* (1.8 pg/m^3)	*Eitzer and Hites*, 1989a
Germany, urban	1993, season is not specified	0.070-0.350	*Fiedler*, 1996
Hamburg, Germany, 8 urban sites	June 1985-October 1986	0.2-1.2* (12-70 pg/m^3)	*Rappe et al*., 1988
Italy, urban	not specified	0.06	*Vozhzennikov et al.*, 1997
Bolsover, UK, 2 km from the industrial complex	October 1992-October 1993	0.31	*Jones and Duarte-Davidson*, 1997
Bolsover, UK, 6 km from the industrial complex	October 1992-October 1993	0.18	*Jones and Duarte-Davidson*, 1997
UK, typical urban air concentration	not specified	0.18	*Duarte-Davidson et al*., 1997
Rotterdam, Netherlands, 10 km from the incinerator	not specified	0.005-0.080	*Vozhzennikov et al.*, 1997
Ausburg, Germany , 7 urban and rural sites	March 1992 - February 1993	0.014 - 0.120	*Hippelein et al*., 1996
Dayton, Ohio, USA, suburban/roadside	Spring 1988	≈ 0.04* (2.2 pg/m^3)	*Tiernan et al*., 1989
UK, typical rural air concentration	not specified	0.04	*Duarte-Davidson et al*., 1997
Germany, rural air concentrations	1993, season is not specified	0.025-0.070	*Fiedler*, 1996
Hamburg, Germany, rural	April 1986	<0.07* (<4 pg/m^3)	*Rappe et al*., 1988

* Calculated assuming that (pg/m^3)/(pg TEQ/m^3) = 60; corresponding concentrations in pg/m^3 are given in brackets.

Table A2 PCDD/F homologue pattern in the atmosphere (ND - concentration of the homologue group is bellow the detection limit)

Reference	*Eitzer and Hites*, 1989b	*Hippelein et al*., 1996	*Tiernan et al*., 1989	*Tierman et al*., 1989
Site	urban, Bloomington, Indiana, USA	7 different sites in Ausburg, Germany	MWI area, Dayton, Ohio, USA	Suburban/roadside Dayton, Ohio, USA
% of TCDF	16	15	6.0	6.0
% of PeCDF	12	11	17	11
% of HxCDF	6.9	7.3	19	6.5
% of HpCDF	3.9	4.1	9.3	5.1
% of OCDF	1.4	2.0	ND	ND
% of TCDD	0.1*	3.6	1.0	ND
% of PeCDD	2.3	5.1	1.7	ND
% of HxCDD	8.1	10	11	2.3
% of HpCDD	19	17	15	19
% of OCDD	31	25	20	50

* - % contribution of this group is underestimated [*Eitzer and Hites*, 1989a]

Table A2 Continuation

Reference	*Rappe et al*., 1988	*Rappe et al*., 1988	*Rappe et al*., 1988	*Vozhzennikov et al.*, 1997
Site	Suburban, Hamburg, Germany	8 urban sites, Hamburg, Germany	2 motorway tunnel sites, Hamburg, Germany	Industrial site, average of 2 samples, Niagara fall, USA
% of TCDF	12	13±9	15±6	13±5
% of PeCDF	17	10±5	12±1	8.6±4.8
% of HxCDF	6.1	9±6	5±2	8.3±3.8
% of HpCDF	3.4	5±3	5±2	7.3±3.1
% of OCDF	ND	2±2	ND	3.2±0.2
% of TCDD	3.4	3±3	0.7	3±3
% of PeCDD	1.7	3±2	6±3	3.5±3.2
% of HxCDD	25	10±5	15±10	6±5
% of HxCDD	20	20±16	11	16±4
% of OCDD	13	23±10	20	31±23

Table A2 Continuation

Reference	*Vozhzennikov et al.*, 1997	Average value ± standard deviation
Site	Industrial site, average of 2 samples, Niagara fall, NY, USA	
% of TCDF	9.3±0.2	12±4
% of PeCDF	7.8±0.6	11±3
% of HxCDF	13±1	9±4
% of HpCDF	12±1	6±3
% of OCDF	4.1±0.1	2.5±1.1
% of TCDD	0.4±0.1	2±1
% of PeCDD	2.1±1.5	3.2±1.6
% of HxCDD	11±1	11±6
% of HpCDD	20±1	17±3
% of OCDD	20±2	22±14

Table A3 Percent contribution of the 2378-substituted congeners to their homologue group

Reference	*Hippelein et al.*, 1996	*Konig et al.*, 1993	*Hagenmaier et al.*, 1993	*Tiernan et al.*, 1989
2378-TCDF/ΣTCDF	5.6±1.5	6.3	4	8.9
12378/12478-PeCDF/ΣPCDF	7.1±1.5	9.3	5	9
23478-PeCDF/ΣPeCDF	7.7±1.5	8.8	6	10
123478/123479-HxCDF/ΣHxCDF	11±3.0	18	18	9
123678-HxCDF/ΣHxCDF	8.2±1.4	10	15	18
234678-HxCDF/ΣHxCDF	11±3.0	8.1	12	ND
1234678-HpCDF/ΣHpCDF	55±3.0	75	60	65
1234789-HpCDF/ΣHpCDF	8.7±1.7	5.3	10	4.4
2378-TCDD/ΣTCDD	3.0±1.1	3.1	ND	ND
12378-PeCDD/ΣPeCDD	5.1±1.1	8.8	12	26
123478-HxCDD/ΣHxCDD	4.8±1.5	4.5	8	8
123678-HxCDD/ΣHxCDD	7.1±1.6	10	15	16
123789-HxCDD/ΣHxCDD	6.7±1.5	7.4	8	12
1234678-HpCDD/ΣHpCDD	53±8.0	55	46	54

Table A4 PCDD/F concentration in soil (w.w. - wet weight, d.w. - dry weight)

Site	Depth of sampling	Sampling period	Concentration	Reference
Tartu, Estonia	5-15 cm	not specified	198 pg/g w.w.	
Rakvere, Estonia	5-15 cm	not specified	61 pg/g w.w.	
Saaremaa Island, Estonia	5-15 cm	not specified	138 pg/g w.w.	
Tallinn, Estonia, city center	5-15 cm	not specified	148 pg/g w.w.	*Brzuzy and*
Tallinn, Estonia, suburban	5-15 cm	not specified	285 pg/g w.w.	*Hites*, 1995
Riga, Latvia	5-15 cm	not specified	93 pg/g w.w.	
Riga, Latvia	5-15 cm	not specified	99 pg/g w.w.	
Vilnius, Lithuania	5-15 cm	not specified	123 pg/g w.w.	
Gorky park, Moscow, Russia	5-15 cm	not specified	377 pg/g w.w.	
Ufa, Russia	not specified	not specified	1-20 pg TEQ/g d.w.	*Vozhzennikov et al.*, 1997
Sterlitamak, Russia	not specified	not specified	1-3 pg TEQ/g d.w.	
UK, urban	not specified	not specified	26 pg TEQ/g d.w. 4660 pg/g d.w.	*Duarte-Davidson et al.*, 1997
5 cities, UK	5cm	not specified	600 - 10000 pg/g d.w.	*Creaser et al.*, 1990
86 rural and suburban sites, UK	5 cm	not specified	453 pg/g d.w. (average value)	*Creaser et al.*, 1989
Sweden, 9-44 km from the center of Stockholm, 30 m from a major road	15-25 cm	May 1989	1.58 pg TEQ/g d.w. (≈ 140 pg/g d.w.)	*Broman et al.*, 1990
Sweden, 8-41 km from the center of Stockholm, 0.5-4 km from a major road	15-25 cm	May 1989	0.98 pg TEQ/g d.w. (≈ 90 pg/g d.w.)	*Broman et al.*, 1990
UK, rural	not specified	not specified	3.3 pg TEQ/g d.w. 324 pg/g d.w.	*Duarte-Davidson et al.*, 1997

Table A5 PCDD/F homologue pattern in soil

Reference	*Creaser et al*., 1990	*Creaser et al*., 1990	*Creaser et al*., 1989	*Broman et al*., 1990	*Broman et al*., 1990
Site, depth of sampling	UK, London 5 cm, site 1	UK, London 5 cm, site 2	UK, rural and suburban sites, 5 cm	Sweden, 9 km from the center of Stockholm, 15-25 cm	Sweden, 26 km from the center of Stockholm, 15-25 cm
% of TCDF	16	0.13	5.5	17	5.7
% of PeCDF	11	0.09	5.1	14	7.9
% of HxCDF	8.6	0.09	9.1	13	5.4
% of HpCDF	3.7	0.42	5.7	2.6	1.1
% of OCDF	2.3	1.0	6.0	ND (<0.5)	ND (<0,05)
% of TCDD	3.7	0.04	2.1	5.8	3.8
% of PeCDD	3.7	0.06	1.5	14	8.3
% of HxCDD	6.3	0.2	8.3	12	6.1
% of HpCDD	13	5.2	15	11	16
% of OCDD	31	93	42	10	46

Chapter 2 Accumulation of persistent organic pollutants by vegetation

B.N.Moisseev

Preface

An attempt is made here to find a relationship between the atmospheric pollution by POPs and their accumulation in vegetation. Due to the scarce experimental materials available, particularly for Eastern Europe, the author had to use a correlation analysis with arbitrary assumptions. We, however, present this work not only to provoke discussion, but also to promote research and mutual information exchange in this poorly studied field.

Introduction

As it is known terrestrial vegetation, first of all forests, can noticeably affect the atmospheric transport and deposition of persistent organic pollutants (POP) due to sorption and assimilation processes. Besides, plants are capable to keep absorbed substances for a long period of time preventing from their secondary emission to the atmosphere.

The uptake of gaseous POP by leaves is described in many publications. A very important result of these studies was the development of the so-called "fugacity" model suggested by D.Mackay in 1979 and elaborated in works by *D.D.Baldocchi* et al. [1987], *M. Riederer* [1990], *D.Mackay* [1991], *S.Paterson et al.* [1991], *H.Hauk et al.* [1994], *G. Deinum et al.* [1995], *M.S.McLachlan* [1996]. The model presumes to achieve a certain steady - state situation between the atmospheric gaseous medium and dissolved gases in a leaf volume. Tentative runs of the "fugacity" model demonstrated reasonable results [*TNO-MEP-Report*, 1996, *TNO-MEP-Report*, 1997]. The accumulation and systematization of data on physical-chemical parameters of pollutants and exchange coefficients between environmental compartments are essential results of this work. However, the problem of POP uptake by the vegetation the penetration of aerosol forms, proportion of accumulation in wood and bark of tree trunks, re-emission rate, degradation and transformation of POP in plants are not sufficiently studied. In this context it is evident that the vegetation should be described by an individual ecosystem module of the model for the atmospheric transport and deposition of POP.

The objective of this work is to estimate the required parameters and “fugacity” model coefficients for approximative calculations of POP fluxes in the "atmosphere - plant -soil" system using data of background monitoring network for Eastern Europe.

Considered organic pollutants: γ-HCH-lindane, ΣDDT, ΣPCB - polychlorinated biphenyls and B(a)P - benz(a)pyrene.

Main tasks:

a) to present initial data and regression equations of a possible connection of POP mean content in assimilating plant organs (leaves, needles, various grass) with mean content of POP in the atmospheric air of background regions;

b) to determine coefficients of the long-term accumulation of POP in the green mass of trees as a relative fraction of depositions;

c) to calculate gas-phase of POP leaf uptake fluxes using stationary version of the "fugacity" model;

d) to calculate POP root uptake fluxes and its ingress to leaves/needles;

e) to estimate POP degradation fluxes in plant;

f) to make a comparative analysis and to determine a systematic error of model calculations of POP concentrations in the green mass of trees.

In many ways, the work presented is of a research (pilot) character and does not claim to be complete and finished. As far as information is accumulated results can be refined and complemented.

1 Methodological approach

Published results of observations at the stations of the Eastern Europe background monitoring [*Rovinsky et al.*, 1988; *Rovinsky et al.*, 1990] were used as initial data. These do not contain the time of vegetation, air, water, and soil sampling.

Again, some of the data were averaged for the whole country or a large region, which makes the initial material considerably less valuable. We believe, however, that for the purpose of modelling on a regional scale, these data are quite appropriate at the first stage of the work since to some extent, they make up for the lack of information for background regions of Eastern Europe.

Correlation and regression analyses were made for data of background monitoring stations. Phyto-accumulation coefficients of POP were determined as a quotient from division of POP flux uptaken by vegetation on dry and wet deposition.

The calculation of POP uptake in the gas-phase was made on the basis of the "fugacity" approach for fluxes in the stationary state [*Riedeer*, 1990; *Deinum et al.*, 1995]. In the model, the concentration of the absorbed matter in leaves is directly proportional to its concentration in the air and is inversely proportional to the leaf-surface resistance. With the concentration in the air known, the problem reduces to seeking an analytical form of resistance with regard to the factors affecting the uptake flux.

Using the balance equation of main mass fluxes in the vegetation module of terrestrial ecosystems of type: $L_{up}+R_{up}=De+Acc$ (where L_{up} - the gas-phase of POP assimilation (leaf uptake) by photosynthesizing organs of plants; R_{up} - root uptake from soil; De - metabolic degradation in plants) estimated from the long-term POP accumulation in green organs of plants - Acc.

Root uptake and POP degradation were calculated with the procedure developed by *D.J.Bakker and W.de Vries* [1996].

Errors of model estimates were analysed by the comparison with measurements of background monitoring stations.

Within the framework of the accepted methodological approach and available data the following assumptions were made:

a) plants uptake only POP available in air in the gaseous form and dissolved in soil water;
b) POP uptaken by roots and leaves are accumulated only in green organs of plants (leaves, needles, green branches and stalks).
c) POP concentrations in leaves and in the air attain a stationary state at the end of the vegetation period;
d) POP degradation in plants takes place with the rate equal to their degradation rate in soil.

2 Analysis of data of background monitoring stations

Systematic routine measurements of pollutants in natural environmental objects carried out at Integrated background monitoring stations (IBMS) of the former USSR make a good information base for the evaluation of the impact of some persistent organic pollutants (POP) on vegetation and ecosystems on the whole. Monitoring stations are located in remote regions with minimum anthropogenic activity for this region. Most commonly it is reserve territories including biosphere reserves. First routine measurements of DDT and some other POP contents in the atmospheric air, surface waters, soil and vegetation were carried out in the former USSR at Borovoe station in 1976. Routine observations of POP content in natural compartments were carried out in European region at background stations in Berezinsk, Prioksko-Terass, Astrakhan, Caucasian and Central-forest biosphere reserves (BR) as well as in cooperative field experiments at background stations in Eastern Europe; in Central Asian region - at background stations in Chatkalsk, Repetek, Sary-Cheleksk, Barguzinsk BR, at stations Borovoe and at high-mountain station Abramov Glacier on Pamir-Alae [*Rovinsky et al.*, 1990].

The pollution of plants by POP of background regions is mainly conditioned by regional and global transports of these substances from places of their application (DDT, lindane) or emissions (PCB, B(a)P). In background regions POP concentrations slightly differ from each other. Averaged values of POP background monitoring data for 1980 - 1987 at stations and in some countries are presented in Table A1-A4 (Annex A). Data on DDT, lindane and PCB were taken from *F.Ya.Rovinsky et al.* [1990]. Data on B(a)P were compilated from *F.Ya.Rovinsky et al.* [1988].

Observational results for PCB are given from only West-European literature since at the background monitoring stations of Russia, PCBs are nearly always available in concentrations beyond the analytical limit of detection.

In order to determine statistical connections, correlation and regression analyses were made using the program STATGRAPHICS, v.5.

2.1 Correlation and regression analysis

In this section the following abbreviations were used:

n - number of sampling,
VEG - substance concentration in plants,
SOIL - concentration in soil,
AIR - concentration in air,
WATER - concentration in surface water,
DEP - dry and wet deposition,
WET - wet deposition,
PRE - concentration in precipitation.

Correlation matrices of station data on POP considered are given in Table 2.1-2.4:

Table 2.1 Correlation matrix of data on DDT (n=27)

	DDT_VEG	DDT_SOIL	DDT_AIR	DDT_WAT	DDT_DEP
DDT_VEG	1.000	0.418	0.041	0.158	-0.089
DDT_SOIL	0.418	1.000	-0.276	0.012	-0.294
DDT_AIR	0.041	-0.276	1.000	0.473	0.913
DDT_WAT	0.158	0.012	0.473	1.000	0.559
DDT_DEP	-0.089	-0.294	0.913	0.559	1.000

Correlation connection DDT-VEG appeared to be very poor with all parameters, i.e. correlation coefficient - $r < 0.7$.

Table 2.2 Matrix of lindane correlation data (n=26)

	LIN_VEG	LIN_SOIL	LIN_AIR	LIN_WET	LIN_WAT	LIN_DEP
LIN_VEG	1	-0.027	0.762	0.635	0.209	-0.080
LIN_SOIL	-0.027	1	-0.049	0.001	-0.245	0.157
LIN_AIR	0.762	-0.049	1	0.416	0.067	-0.095
LIN_WET	0.635	0.001	0.416	1	0.023	-0.218
LIN_WAT	0.209	-0.245	0.067	0.023	1	0.225
LIN_DEP	-0.080	0.157	-0.095	-0.218	0.225	1

The correlation between lindane content in the air and vegetation is rather close (r=0.762).

Table 2.3 Matrix of PCB data correlation (n=16)

	PCB_VEG	PCB_SOIL	PCB_AIR	PCB_WAT	PCB_PRE	PCB_DEP
PCB_VEG	1	0.8836	0.8471	0.0750	0.8532	0.8963
PCB_SOIL	0.8836	1	0.8021	0.3097	0.9040	0.9083
PCB_AIR	0.8471	0.8021	1	-0.0066	0.8221	0.8243
PCB_WAT	0.0750	0.3097	-0.0066	1	0.4587	0.3417
PCB_PRE	0.8532	0.9040	0.8221	0.4587	1	0.9837
PCB_DEP	0.8963	0.9083	0.8243	0.3417	0.9837	1

The very close correlation of PCB-VEG with PCB content in soil, air and precipitation and with total deposition ($r > 0.8$) is surprising. May be such a connection is likely to be an artefact since our sampling contains only averaged data for the countries obviously with very smoothed deviations.

Table 2.4 Matrix of B(a)P data correlation (n=16)

	BAP_VEG	BAP_SOIL	BAP_AIR	BAP_WAT	BAP_DEP
BAP_VEG	1	0.6244	0.2963	0.2793	0.8693
BAP_SOIL	0.6244	1	0.5154	0.695	0.6041
BAP_AIR	0.2482	0.5154	1	0.4287	0.6201
BAP_WAT	0.2776	0.695	0.4287	1	0.3206
BAP_DEP	0.8693	0.6041	0.6201	0.3206	1

It is in clear that there is no correlation between BAP_VEG and its concentration in air, since according to literature data B(a)P is present in air in the aerosol phase. Obviously due to this fact a close link between its content in vegetation and total deposition ($r = 0.869$) is manifested.

To make a qualitative support of the correlation analysis results and their possible use in model calculations the regression analysis of the essential correlations was made:

Lindane

$$Y = 3.76 + 13.91 \times X \quad (r = 0.762; \quad SEE = +/- 4.54) \qquad (1)$$

where: Y - lindane concentration in plants, ng/g;
X - lindane concentration in the atmospheric surface layer, ng/m^3,
r - pair correlation coefficient,
SEE - standard estimate of errors, ng/g.

PCB

$$Y = 11.79 + 29.85 \times X \quad (r = 0.847; SEE = +/-25.77) \qquad (2)$$

where Y - PCB concentration in plants, ng/g;
X- PCB concentration in the atmospheric surface layer, ng/m^3.

B(a)P

$$Y = -0.101 + 4.67 \times X \quad (r = 0.86; \quad SEE = +/-1.62) \qquad (3)$$

where Y - B(a)P concentration in plants, ng/g;
X - B(a)P total deposition, g/ha×yr.

Regression links of BAP_VEG with BAP_SOIL are as follows:

$$Y = 1.34 + 0.778 \times X \quad (r = 0.624; \quad SEE = +/-2.48) \qquad (4)$$

where Y - B(a)P concentration in plants, ng/g;
X - B(a)P concentration in soil layer, ng/g.

2.2 POP long-term accumulation in the green mass of plants

An important indicator of the role of plants in the balance of POP fluxes is so-called bioaccumulation factor (BCF) which is in close correlation with the distribution coefficient of octanol-water [*Bacchi et al.,* 1990]. It is determined by a simple ratio of POP concentration in plants (C_V) to its concentration in air (C_A) for a steady-state situation:

	C_V ($\times 10^6$), ng/m^3	C_A, ng/m^3	BCF ($\times 10^6$)
DDT	1.28	0.40	3.2
LINDANE	0.44	0.32	1.4
PCB-153	1.35	0.93	1.5
B(a)P	0.17	0.25	0.7

However, BCF is difficult to interpret properly, since a concentration in plants usually expressed in mass units per mass unit it is necessary to convert to dimensions of mass unit per volume unit but in doing so the sense is lost because it is difficult to present leaves of trees in volumetric units (in such dimensions BCF is used in some model calculations as the plant-air partition coefficient). Therefore we suggest another integral indicator (K_{acc} - phyto-accumulation coefficient), which is determined as: K_{acc}=Acc/Dep, where Acc- long-term flux of POP accumulation in the green mass of plants, g/ha×yr; Dep- POP dry and wet depositions, g/ha×yr. Physical sense of K_{acc} is evident. This coefficient can be directly used in model calculations of POP transport and deposition, as well as in calculations of critical loads.

A long-term flux of POP accumulation in the plant green mass was calculated in the following way:

$$Acc(POP) = 0.001 \times C_V \times F_{green} \times NPP \qquad (5)$$

where: Acc(POP) - POP accumulation, g/ha×year;
C_V - POP concentration in green mass, ng/g;
F_{green} - coefficient considering the fraction of green mass in NPP (≈0.4);
NPP - net primary production d.w., ton/ha×yr.

NPP estimates used in calculations are given in table A5 (Annex A). Calculation results of deposition fluxes, POP accumulation (g/ha×yr) and phyto-accumulation coefficients for monitoring stations are given in table A6 (Annex A).

Mean values of phyto-accumulation coefficients, (K_{acc}), in our sampling are as follows:

K_{acc}(DDT) = 0.13+/-0.028
K_{acc}(LIN) = 0.26+/-0.059
K_{acc}(PCB) = 0.031+/-0.005
K_{acc}(B-a-P) = 0.013+/-0.0075

As seen from the obtained fluxes of PCB and B(a)P long-term accumulation by the vegetation in background regions do not play an essential role in the general mass balance. However *S.L.Simonich and R.A.Hites* [1994] believe that 1/2 of all PAH fluxes comes through vegetation. The authors considered PAH aerosol fraction which is sorbed in great quantities on the area of leaves/needles and tree bark. Nevertheless Bromstrom-Lunden [*TNO-MEP-Report*, 1996] came to a conclusion that PAH are uptaken by the surface of plants and they rapidly degrade under the impact of light and ozone. Thus, the published data on the vegetation impact on the B(a)P transport in the atmosphere are rather contradictory. This problem requires further research.

3 Model calculation

As it is known POP enter a plant via leaves/needles, via epidermis of stems and branches and by root uptake from the soil solution. It was found in many investigations [*Gaggi et al.,* 1986; *Bacci et al.*, 1990; *Trapp et al.*, 1990; *McLachlan*, 1996; *Hauk et al.*, 1994; *Paterson et al.*, 1994; *Strachan et al.*, 1994] that such lipophylic ($\log K_{ow}>4$) water insoluble compounds as DDT, PCB, B(a)P are unlikely to penetrate to vegetation from soil. Whereas water-soluble HCH ($\log K_{ow} < 4$) isomers are capable to penetrate to plants through the root system and to be accumulated in green organs. An essential input of POP aerosol produced via epidermis is possible only in the case of their high concentrations in air [*Trapp at al.*, 1990] but it is not considered in this work.

3.1 Assimilation of gaseous POP from the atmosphere

The input of gaseous POP from the atmosphere takes place through stomata and cuticle. At night stomata are semi-closed and an intensive flux of CO_2 - carbon dioxide and water vapors come out of them. Therefore the night-time input of POP to leaf mesophyll is realized via cuticle. The most detailed and complete description of the model of POP stomatal uptake considering a great number of input parameters is presented in the paper by *D.D.Baldocchi et al.* [1987]. A simpler model of stomatal uptake was developed by *S.B.Jdso* [1988] and *M.Riederer* [1990]. *S.Paterson et al.* [1994] have developed so-called "fugacity model" where a leaf volume is divided into water, air and “octanol" (lipids). The next level of this model considers POP transport and transformation in leaf during a given time period [*Paterson et al*., 1994; *McLachan et al.*, 1996; *Hauk et al.*, 1994; *Deinum et al.*, 1995].

In our model calculations the following mean values of coefficients of POP distribution between gas and aerosol phases in the atmosphere of background regions are taken:

DDT	K_g=0.6 [*Rovinsky et al.,* 1990];
Lindane	K_g=0.9 - " -
PCB	K_g=1.0 [*Progress report*, 1997];
B(a)P	K_g=0.1 [*Rovinsky et al.,* 1988].

It should be mentioned that according to data of *F.Ya.Rovinsky et al* [1990] a relative fraction of PCB gaseous form in the atmosphere varies in a wide range from 40% to 100%.

The flux of gaseous POP to leaves through stomata + cuticle (for 15 daytime hours) and cuticle (for 9 night 9 hours) for the whole vegetation period was calculated using a modified formula [*Deinum et al.*, 1995]:

$$L_{up}(POP) = \frac{10000 \cdot LAI \cdot t}{R_T} \cdot (F_g \cdot C_A - C_L / K_{la}) \qquad (6)$$

where L_{up}(POP) - POP flux to leaves, g/ha during the vegetation period;
LAI - leaf area index , m^2/m^2;
R_T - total resistance of the air boundary layer, stomata+cuticle (in the daytime) and only cuticle (at night), s/m;
t - total duration of the daytime light period (t = 60×60×15×180 s for stomata + cuticle) and the night-time period (t = 60×60×9×180 s for cuticle) at the vegetation period (≈180 day);
F_g - partition coefficient between POP gaseous and aerosol phases;
C_A - POP mean equilibrium air concentration (C_A = constant), g/m^3;
C_L - POP concentration in the volume of leaves, g/m^3;
K_{la} - leaves-air partition coefficient.

It is evident that at the beginning of the vegetation period POP concentration in leaves is close to zero. Besides numerical value of K_{la} is very high (according to TNO-MEP-R97/150 - more than 10^5) therefore in the first approximation C_A/K_{la} in eq.(6) is assumed to be zero. However *J.H.Duyzer et al*. [1996] in laboratory experiments found that the uptake rate decreases with mesophyll saturation with POP.

The total resistance of leaves in the daytime was obtained from formula [*TNO-MEP-Report*, 1997]:

$$R_T = R_b + \frac{1}{R_s^{-1} + R_c^{-1}}, \qquad (7)$$

where R_b - resistance of the air boundary layer (=100 s/m, according to *M.Riederer* [1990];
R_s - stomatal resistances (at night R_s=0), s/m;
R_c - cuticle resistance, s/m.

Stomatal resistances were estimated as [*Baldocchi et al*., 1987]:

$$R_s = R(H_2O) \times [M/M(H_2O)]^{1/2} \quad (8)$$

where $R(H_2O)$ - stomatal resistances to water vapor (=1000 s/m, according to *M.Riederer* [1990];
M and $M(H_2O)$ - molecular mass of POP and water respectively, g/mol.

Calculation results of stomatal resistances are as follows:

	M, g/mole	$R_s \times 10^3$, s/m
DDT	354.0	4.4
LINDANE	290.8	4.0
PCB-153	360.7	4.5
B(a)P	252.3	3.7

Cuticlar resistances were estimated as [*Sabljic et al.,* 1990]:

$$\log R_c = \log(H/R_T) - 0.734 \times \log K_{cw} + 11.26 \quad (9)$$

where $H/R_T = K_H$ - Henry' law constant (-);
K_{cw} - cuticle/water partition coefficient ($\log K_{cw} = 0.57 + 0.97 \times \log K_{ow}$).

Table 3.1 presents initial data and calculation results by formula (9).

Table 3.1 Calculation results of cuticular resistance and total resistance

	$\log K_{cw}$	$\log(H/R_T)$	$R_c \times 10^3$, s/m	$R_T \times 10^3$, s/m
DDT	6.06	-2.82	9.8	3.1
LINDANE	3.74	-3.87	43.9	3.8
PCB-153	6.85	-2.43	6.3	2.6
B(a)P	5.88	-4.72	2.2	1.4

For B(a)P cuticle resistance appeared to be lower than that of stomatal resistence.

Octanol-water partition coefficients were assumed as:

DDT	[*TNO-MEP- Report*, 1997]	$\log K_{ow} = 6.2$
LINDANE	[*ESQUAD project*, 1994]	$\log K_{ow} = 3.8$
PCB-153	[*Rioderer,* 1990]	$\log K_{ow} = 7.0$
B(a)P	[*ESQUAD project,* 1994]	$\log K_{ow} = 6.0$

Henry's law constants were assumed as:

DDT	K_H = 1.5e-3 [*Holoubek et al.*, 1993]	$\log K_H$ = -2.82
LINDANE	K_H = 1.3e-4 [*Bakker et al.,* 1994]	$\log K_H$ = -3.87
PCB-153	K_H = 3.7e-3 - ″ -	$\log K_H$ = -2.43
B(a)P	K_H = 1.9e-5 [*Holoubek et al,* 1993]	$\log K_H$ = -4.72

Using literature data [*Utkin*, 1975] the correlation connection of net primary production, NPP, of boreal forests ETR with leaf area index, LAI, can be expressed by the regression equation:

$$LAI = \exp(0.760 + 0.072 \times NPP), \quad (10)$$

r = 0.739; SEE = +/-0.271. Here $2 < NPP < 15$ tons/ha.

Quantitative relationships of the green mass of trees, M_{green}, LAI and NPP, are approximately as follows:

$$M_{green} \approx 10000 \times LAI \times z \times \rho \approx 0.4 \times NPP \quad (11)$$

where M_{green} = stock of green biomass of tree stand, ton/ha;
z = 0.0015 m - assumed mean thickness of a leaf;
ρ = 0.05 ton d.w./m^3 - density of leaves/needles assumed in calculations.

It should be mentioned that in the end of the vegetation period POP uptaken by leaves come to the litter and in 5...15 years - to the soil. It is self-evident that during long periods of time this cycle is continuously realized.

The following estimates mean values of POP assimilation fluxes calculated by the stationary "fugacity" model (6) were obtained (g/ha) during the vegetation period:

	Daytime	Night	Total
DDT	0.030	0.006	0.036
LINDANE	0.031	0.002	0.033
PCB – 153	0.148	0.036	0.184
B(a)P	0.006	0.002	0.009

As seen from the data, the greatest fraction of night assimilation is found for B(a)P (22%), the least one - for lindane (6%) as it follows from physical-chemical properties of these substances.

Model assessments of POP assimilation fluxes for background monitoring stations are given in tables A7-A10 (Annex A).

3.2 POP root uptake

Under natural conditions POP high sorption capacity results in the concentration of the bulk of these substances in the lower and the upper soil layer (0...20 cm) after a long lapse of time

[*Gaggi et al.*, 1986]. A certain part of these substances enters the soil solution and can penetrate to plants via the root system. POP flux uptaken by roots and coming to leaves through xylem was calculated using formula [*Bakker and de Vries,* 1996]:

$$R_{up}(POP) = K_{up} \times E_t \times C_w \quad (12)$$

where R_{up} - POP uptake by roots, g/ha during the vegetation period;
K_{up} - preference coefficient (-);
E_t - water consumption at plant transpiration (≈40% of total evaporation), m^3/ha;
C_w - POP concentration in the soil solution (surface water), g/m^3.

Preference coefficients were calculated by formula [*Briggs et al.,* 1983]:

$$K_{up} = 0.784 \times \exp-[(\log K_{ow}-1.78)^2/2.44] \quad (13)$$

where K_{ow} -octanol-water partition coefficient.

For lipophil substances $K_{up}<1\times10e^{-4}$, i.e root uptake fluxes of DDT, PCB, B(a)P are inessential and they can be excluded from calculations. It is known from publications [*Hulster et al.,* 1994; *McLachlan,* 1996], that lipophil substances are almost completely sorbed by root epidermis and later they do not penetrate into a plant.

For lindane the preference coefficient appeared to be equal to 0.15. Calculations by formula (12) showed that on the average the flux of lindane uptake by roots is 0.003 g/ha or about 10% of the assimilation flux by leaves from the atmosphere (table A8 (Annex A)).

3.3 Approximative estimates of POP degradation in plants

Photochemical reactions and processes of metabolic decay with the participation of micro-organisms may be considered the most common mechanism of POP degradation in the environment. Photochemical reactions take place not only in the atmosphere but also at the interface boundaries: air-soil, air-plant. It should be mentioned that due to low rate of POP decay in vegetable material, POP content in vegetation is several times higher than the observed levels of concentrations in soils [*Rovinsky et al.,* 1990].

In the literature reviewed no data on POP degradation rate in plants were found therefore in model calculations the degradation rate in soil [*Harper et al.,* 1983] was assumed which constants are given in table 3.2.

Table 3.2 Assumed POP degradation constants

	K_{deg}, 1/yr (from literature)	$0.5\cdot K_{deg}$, 1/yr (assumed)
DDT	0.03 – 0.1 [*Bobovnikova et al*., 1988]	0.03
LINDANE	0.243 [*Lunev and Tsukermann,* 1987]	0.12
PCB-153	0.07 [*Bakker et al.,* 1994]	0.04
B(a)P	0.041 [*Bakker et al.,* 1994]	0.02

Since our calculations were made for the vegetation period, degradation coefficients (1/yr) were twice reduced. As evident from values presented, lindane degradation coefficient is of an actual significance for mass fluxes.

The degradation flux in plants was calculated from formula:

$$De(POP) = 0.5K_{deg} \times (L_{up} + R_{up}) \quad (14)$$

where De(POP) - degradation flux in plants, g/ha during the vegetation period;
K_{deg} - degradation rate constant, 1/yr.

The obtained mean value of flux De(Lin) is equal to 0.0043 g/ha×per. It accounts for about 10% of the total uptake of lindane by roots (table A8 (Annex A)). Mean values for DDT and PCB degradation fluxes are very small - 0.001 and 0.004 g/ha respectively and for benz(a)pyrene this flux is practically equal to zero.

Thus mean (approximative) values of POP fluxes coming through plants at background monitoring stations are the following (g/ha during the vegetation period):

	L_{up}	R_{up}	De
DDT	0.036	0	0.001
LINDANE	0.033	0.003	0.0043
PCB-153	0.184	0	0.004
B(a)P	0.009	0	0

3.4 Model errors and uncertainties

1. The greatest uncertainty is caused by the initial data of background monitoring stations and by their averaged estimates for countries and regions.
2. Calculations of POP mass fluxes using a simple "fugacity" model demonstrated a good approximation to measurement (and recalculated for a flux) data:

	Acc, g/ha×yr (mean for measurements)	Acc,g/ha×yr (mean for model)	Mean model error, g/ha×yr	Mean model error,%	Corr.coeff Mod./Meas.
DDT	0.070	0.036	- 0.032	- 45.7	0.81
LINDANE	0.029	0.031	+ 0.003	+10.3	0.80
PCB-153	0.160	0.184	+ 0.023	+14.4	0.71
B(a)P	0.012	0.009	- 0.003	- 25.0	0.77

It is interesting that the correlation coefficient of measured and calculated accumulation of DDT appeared to be the highest (r = 0.81) in spite of the fact that the relative model error for this substance is the greatest.

The comparison of measured and calculated POP concentrations in plants demonstrated somewhat different results:

	C_V, ng/g (mean for measurements)	C_L, ng/g (mean for model)	Mean model error , ng/g	Mean model error ,%
DDT	26	8.7	-15.5	- 64.6
LINDANE	9	8.0	- 0.8	- 8.9
PCB-153	39	57.5	+ 18.1	+46.4
B(a)P	3.4	2.3	- 1.03	- 30.7

The model does not consider the penetration of part of dissolved in water POP into leaves and stalks therefore underestimated results probably were obtained for DDT and B(a)P. A portion of the gas form of PCB-153 requires refinements.

3. The calculations were made with the stationary version of the "fugacity" model which does not allow to detect the dynamics of concentrations and the decrease of POP penetration rate into leaves during the vegetation period.

4. Unfortunately in literature there are no data on re-emission rate and POP degradation in plants. Probably photo-degradation rate is rather essential in leaves particularly for B(a)P.

5. Only data on background monitoring are used in our sampling. For the evaluations of the impact of POP more extensive database is required.

6. The comparison of POP uptake by different types of vegetation has not been made. As follows from eq.(6) the mass of POP assimilation fluxes depends on LAI. Judging by literature data the most typical estimates of LAI are the following: deciduous forests=2...5, coniferous forests=3...8, grasslands and crops=5...20 m^2/m^2.

Conclusions

With respect to calculations made on the basis of data of background monitoring stations the following conclusions can be drawn:

- the correlation of lindane and PCB content in plants (i.e. for substances with a large fraction of gaseous forms in the atmosphere) with the concentrations in air appeared to be rather high ($r > 0.7$), whereas for DDT and B(a)P the correlation is low ($r < 0.3$);

- in background regions the long-term accumulation of PCB and B(a)P by vegetation do not play an essential role in a general mass balance;

- calculation of POP assimilation by leaves using the stationary version of "fugacity model" showed a reasonable agreement of calculated and measured values;

- for lipophilic chemicals (DDT, PCB, B(a)P) fluxes of root uptake are insignificant and can be neglected in mass balance calculations;

- estimates of POP bioconcentration and degradation rates in plants are very uncertain and require further examination.

A balance model and quantitative estimates of POP in the "atmosphere - plant - soil" system are needed for the evaluation of POP transport.

Glossary of some biological terms

Xylem - water conducting tissue of wood vessel plants**.** Together with **phloem** it forms a conducting system combining all organs of plants.

Cuticle - a layer of fat substance covering the area of leaves, stalks and fetuses by a solid film. The cuticle complex includes cellulose, pectin, cuticle, wax and other substances and it has layered structure. A net of hydrophilous pectin capillaries runs through the cuticle depth.

Lipids - fat like substances in the content of all living cells. Being one of the main components of biological membranes lipids affect cell perviousness. Lipids are surface active substances moderately soluble in non-polar solvents (petroleum ether, benzene etc.) and weakly soluble in water.

Mesophyll - tissue of a leaf plate between epidermal layers. Due to a developed system of intercells communicating with stomatal vissure mesophyll has a broad internal surface and fulfils the function of gas exchange.

Transpiration - physiological evaporation of water by a plant. The main transpiration organ is a leaf evaporating water through a stoma (90...95%) and cuticle (10...5%). Together with the root pressure transpiration provides a continuous flow of water through roots, stalks and leaves from soil to the atmosphere.

Stomata - specific formation of plant epidermis consisting of two closing cells and intercell (Stoma vissure) between them. Gas exchange required for photosynthesis, respiration and transpiration is realized through the vissure. The number of stomata and their location depends on species and usually vary from 50 to 300 per 1 mm^2 of leaf/needle area.

Net primary production (NPP) - vegetable substance of the ecosystem accumulated during the vegetation period including leaves/needles, foetus/seeds, branches/stalks, wood, roots, living above the soil cover.

Epidermis - ground tissue of leaves, stalks, foetus and seeds often with the external cover of cuticle, wax coating, living and dead hair. Water and nutritious substances penetrate via pores into external walls of cellular membrane. In epidermis closing cells of stomata are formed. Epidermis provides gas exchange, suction and secretion of various substances including enzymes and hormone.

References

Bacci E. et al. [1990] Bioconcentration of organic chemical vapors in plant leaves: experimental measurements and correlation.- Env. Sci. Technol., № 24.

Bakker D.J., de Vries W. [1996] Mannual for calculating critical loads of persistent organic pollutants for soils and surface waters.- TNO-MEP report R 96/509, The Netherlands.

Bakker D.J. et al. [1994] MW-TNO report, R 94/288.

Baldocchi D.D., Hicks B.B. and Camara P. [1987] A canopy stomatal resistance model for gaseous deposition to vegetated canopies. Atmos. Environ., v.21, pp.91-101.

Bobovnikova Ts.I. et al. [1988] Consequences of the airborne long-range transport of chlororganic pesticides and polychlorinated biphenyls. Hygiene and Sanitation, v.7 (in russian).

Briggs G.G., Bromilow R.H., Evans A.A., Williams M. [1983] Relationships between lipophilicity and the distribution of non-ionised chemicals in barley shoots following uptake by the roots. Pestic. Sci., v.14, pp.492-500.

Deinum G. et al [1995] The influence of uptake by leaves on atmospheric deposition of vapor-phase organics.- Atmospheric Env., № 29.

Duyzer J.H. et al [1996] Determination of deposition parameters of a number of POP's by laboratory experiments.- TNO- MEP Report R96/409, Apeldoorn, The Netherlands.

ESQUAD project [1994] van den Hout (ed). The Impact of Atmospheric Deposition of Non-Acidifying Pollutants on the Quality of European Forest Soils and the North Sea. Main report of the ESQUAD project, The Netherlands, p.143.

Harper L.A. et al. [1983] Microclimate effects on toxaphene and DDT volatilization from cotton plants. Agronomy, v.75, pp.295-303.

Hauk H., Umlauf G., McLachlan M.S. [1994] Uptake of gaseous DDE in spruce needles. Env. Science and Techn., v.28, pp.2372-2379.

Holoubek I. et al. [1993] Methodologies for the estimation of the emission of POP's to the atmosphere.- Project TOCOEN.

Hulster A., Muller J.F., Marschner H. [1994] Soil Plant Transfer of Polychlorinated Dibenzo-P-Dioxins and Dibenzofurans to Vegetables of the Cucumber Family (Cucurbitaceae). Environ Sci Technol., v.28, pp.1110-1115.

Gaggi C., Bacci E., Fanelli R. et al. [1986] Chlorinated hydrocarbons in plant foliage: an indication of the tropospheric contamination level. - Chemosphere, v. 15, № 6, pp.747-754.

Jdso S.B. [1988] Development of a simlefiedplant stomatal resistance model and its validation for potentialy transpiring and water-stressed water hyacinths. Atmos. Env., v.22, № 8.

Lunev M.I., Tsukermann V.G. [1987] Degradation of persistent pesticides in soils of various types. Bulletin of the All-Union Scientific Research Institute of Agriculture and Microbiology, v.46, pp.9-11(in russian).

Mackay D. [1991] Multimedia Environmental Models: The Fugacity Approach. - Lewis, Chelsea, MI.

McLachlan M.S. [1996] Bioaccumulation of hydrophobic chemicals in agricultural food chains. Env. Sci. Technol., v.30, pp.252-259.

Paterson S. et al [1991] A fugacity model of chemical uptake by plants from soil and air. Chemosphere, v.23.

Paterson S., Mackay D., McFarlane C. [1994] A model of ogranic chemical uptake by plants from soil and the atmosphere. Env. Sci. Technol., v.28, № 13, pp.2259-2266.

Progress report MSC-E-RIVM [1997] Modelling of long-range transport of lindane and PCB with implementation of RIVM model of atmosphere-surface exchange, August 1997.

Riederer M. [1990] Estimating partitioning and transport of organic chemicals in the follage/atmosphere system: discussion of a fugacity-based model. Environ. Sci. and Technol, v.24, № 6, pp.829- 837.

Rovinsky F.Ya. et al. [1990] Background monitoring of land ecosystem pollution by chlororganic compounds. L., p.270 (in russian).

Rovinsky F.Ya. et al. [1988] Background monitoring of policyclic aromatic hydrocarbons. L. (in russian).

Sàbljic A. et al. [1990] Modelling plant uptake of airborne organic chemicals. 1.Plant cuticle/water partitioning and molecular connectivity.- Env. Sci.Technol., № 24.

Simonich S.L., Hites R.A. [1994] Importance of vegetation in removing polyciclyc aromatic hydrocarbons from the atmosphere. Nature, v.370, pp.49-51.

Strachan et al. [1994] Organoclorine compounds in pine needles: methods and trends.- Env. Toxicology and Chemistry, № 13.

TNO-MEP -Report [1996] (R 96/409) The Netherlands, p.409.

TNO-MEP -Report [1997] (R 97/150) The Netherlands, p.150.

Trapp S. et al. [1990] Modelling the bioconcenttration of organic chemicals in plants. - Env. Sci. Technol., № 24.

Utkin A.I. [1975] Biological productivity of forests. Dendrology and Forestry, v.1, M. (in russian).

ANNEX A

Table A1 ∑DDT content in natural compartments of background regions

Station region	Conc. in vegetation, ng/g	Conc. in soil, ng/g	Conc. in air, ng/m^3	Conc. in water, ng/l	Deposition, g/ha × yr		
					dry	wet	∑
Astrakhan	18	13	0.3	25.0	0.24	0.14	0.38
Berezinsk	20	15	0.4	21.0	0.27	0.56	0.83
	21	15	0.4	78.0	0.27	0.56	0.83
Caucasian	11	7	0.9	80.0	0.76	1.50	2.26
	20	7	0.9	111.0	0.76	1.50	2.26
Prioks_Terr	8	7	0.6	82.0	0.47	0.58	1.05
	7	7	0.6	37.0	0.47	0.58	1.05
Tsentr_Lesnoi	4	10	0.5	4.3	0.39	0.32	0.71
	14	10	0.5	118.0	0.39	0.32	0.71
Barguzinsk	23	20	0.3	56.0	0.22	0.32	0.54
Borovoe	17	8	0.5	24.0	0.36	0.27	0.63
	65	8	0.5	67.0	0.36	0.27	0.63
Repetek	24	27	0.3	50.0	0.22	0.11	0.33
Sary_Chelek	43	25	0.2	20.0	0.19	0.17	0.36
	*(126)	25	0.2	98.0	0.19	0.17	0.36
Chatkalsk	20	14	0.3	4.0	0.30	0.05	0.35
	64	14	0.3	8.0	0.30	0.05	0.35
Abramov Glacier	1	8	0.1	8.0	0.05	0.06	0.11
ETR	12	10	0.5	50.0	0.42	0.59	1.01
	21	10	0.5	70.0	0.42	0.59	1.01
ATR	21	15	0.3	20.0	0.22	0.11	0.33
	85	15	0.3	40.0	0.22	0.11	0.33
E. Europe	30	16	0.8	30.0	0.70	0.38	1.08
	*(160)	16	0.8	50.0	0.70	0.38	1.08
W. Europe	25	10	0.2	50.0	0.08	0.04	0.12
	12	10	0.2	1.0	0.08	0.04	0.12
N. America	28	3	0.1	5.0	0.08	0.02	0.10

*( ) - value are not considered

Table A2 Content of lindane, γ-HCH in natural compartments of background regions

Station region	Vegetation, ng/g	Soil, ng/g	Air, ng/m^3	Precipitation, ng/l	Water, ng/l
Astrakhan	3	3	0.14	20	3
	6	3	0.32	20	40
Berezinsk	1	10	0.15	22	3
	3	10	0.27	22	11
Caucasian	3	3	0.15	30	7
	7	3	0.40	30	68
Prioks_Terr	4	3	0.40	32	20
	18	3	0.50	32	46
Tsentr_Lesnoi	3	2	0.20	4	4
	5	2	0.20	4	21
Barguzin	9	7	0.24	17	39
	4	7	0.10	17	13
Borovoe	5	5	0.30	27	8
	10	5	0.60	27	27
Repetek	14	4	0.30	30	30
Sary_Chelek	10	4	0.22	60	13
	21	4	0.70	160	27
Chatkalsk	10	5	0.25	69	3
	27	5	*(2.00)	69	9
Abramov Glacier	4	4	0.11	12	8
ETR	3	4	0.14	26	23
	7	4	0.50	26	23
ATR	4	5	0.10	57	15
	21	5	0.70	57	15
E.Europe	11	7	0.19	10	14
	17	7	0.32	70	23

*( ) - value are not considered

Table A3 Content of ∑PCB in natural compartments of background regions

Station region	Vegetation, ng/g	Soil, ng/g	Air, ng/m^3	Precipitation, ng/l	Water, ng/l
Sweden	7 34	0.02 1.40	10 15	0 1	10 30
Germany	10 13	0.10 1.00	4 20	24 63	24 63
Norway	15 49	0.18 0.25	10 15	10 20	10 50
Greece	3	0.01	1	1	10
UK	8 14 40	0.01 0.30 1.00	1 8 26	1 10 20	10 30 50
Italy	27 117	0.30 1.00	15 30	10 30	30 60
Yugoslavia	26	0.30	15	10	20
North America	10 88 170	1.00 3.00 5.00	10 25 40	1 5 10	20 60 100

Table A4 Content of B(a)P in natural compartments of background regions

Station	Vegetation, ng/g	Soil, ng/g	Air, ng/m^3	Water, ng/l
Astrakhan	0.40 0.90	0.60 0.90	0.18 0.18	1.00 3.20
Berezinsk	3.00 4.70	1.10 7.00	0.07 0.78	1.00 4.00
Caucasian	2.30 9.90	0.80 3.30	0.03 0.22	1.90 2.50
Prioks_Terr	2.00 3.70	0.18 4.36	0.30 0.90	2.10 4.30
Tsentr_Lesnoi	0.80 8.40	0.80 8.40	0.22 0.22	2.50 4.50
Barguzinsk	1.60 2.70	0.90 1.30	0.02 0.08	2.20 3.50
Borovoe	2.40 8.80	2.00 4.30	0.37 0.37	4.00 4.00
Repetek	5.00	3.00	0.28	4.00
Sary_Chelek	0.10 0.20	0.05 4.90	0.03 0.08	3.20 4.90

Table A5 Estimates of NPP, LAI, precipitation, and evaporation (according to literature data)

Region	NPP, t/ha×yr	LAI, m^2/m^2	PRES, mm/yr	EVAP, mm/yr
Astrakhan	5.0	3.1	300	300
	6.0	3.3	300	300
Berezinsk	8.0	3.8	650	500
	9.0	4.1	650	500
Caucasian	12.0	5.1	1400	600
	14.0	5.9	1400	600
Prioks_Terr	7.0	3.5	650	500
	9.0	4.1	650	500
Tsentr_Lesnoi	6.0	3.3	650	500
	8.0	3.8	650	500
Barguzinsk	5.0	3.1	550	400
	6.0	3.3	550	400
Borovoe	4.0	2.9	350	350
	5.0	3.1	350	350
Repetek	6.0	3.3	600	500
Sary_Chelek	9.0	4.1	950	700
	10.0	4.4	950	700
Chatkalsk	8.0	3.8	750	600
	9.0	4.1	750	600
Abramov Glacier	1.0	0.5	750	400
ETR	7.0	3.5	500	400
	10.0	4.4	800	600
ATR	6.0	3.3	400	300
	8.0	3.8	600	400
East Europe	7.0	3.5	700	500
	10.0	4.4	800	600
West Europe	8.0	3.8	700	500
	10.0	4.4	900	600
Sweden	6.0	3.3	600	400
	9.0	4.1	900	600
Germany	7.0	3.5	600	400
	9.0	4.1	900	600
Norway	6.0	3.3	600	400
	9.0	4.1	1200	500
Greece	10.0	5.1	700	600
UK	8.0	3.8	600	400
	9.0	4.1	800	500
	10.0	4.4	1000	600
Italy	10.0	4.4	600	500
	14.0	5.9	1200	700
Yugoslavia	12.0	5.1	800	600
North America	7.0	3.5	700	400
	8.0	3.8	800	500
	10.0	4.4	900	600

Table A6 Deposition, POP accumulation (g/ha×yr) and phyto-accumulation coefficient

(calculations are made on the bases of literature data)

	DDTdep	DDTacc	DDT_K	LINdep	LINacc	LIN_K	PCBdep	PCBacc	PCB_K	BAPdep	BAPacc	BAP_K
Astrakhan	0.38	0.02	0.05	0.05	0.006	0.12				0.2	0.001	0.005
	0.38	0.06	0.16	0.15	0.014	0.09				0.4	0.002	0.005
Berezinsk	0.83	0.06	0.07	0.10	0.003	0.03				0.5	0.010	0.020
	0.83	0.08	0.10	0.20	0.011	0.05				1.5	0.017	0.011
Caucasian	2.26	0.05	0.02	0.02	0.014	0.70				0.5	0.011	0.022
	2.26	0.11	0.05	0.05	0.039	0.78				2.0	0.055	0.028
Prioks_Terr	1.05	0.02	0.02	0.10	0.011	0.11				0.5	0.006	0.012
	1.05	0.03	0.03	0.20	0.065	0.33				1.5	0.013	0.009
Tsentr_Lesnoi	0.71	0.01	0.01	0.05	0.007	0.14				0.2	0.002	0.010
	0.71	0.04	0.06	0.10	0.016	0.16				1.0	0.027	0.027
Barguzinsk	0.54	0.03	0.06	0.20	0.018	0.09				0.5	0.003	0.006
	0.54	0.09	0.17	0.20	0.010	0.05				0.5	0.006	0.012
Borovoe	0.63	0.03	0.05	0.23	0.008	0.03				0.5	0.004	0.008
	0.63	0.13	0.21	0.23	0.020	0.09				1.5	0.018	0.012
Repetek	0.33	0.06	0.18							1.0	0.012	0.012
Sary_Chelek	0.36	0.15	0.42									
	0.36	0.17	0.47									
Chatkalsk	0.35	0.06	0.17									
	0.35	0.07	0.20									
Abramov Glacier	0.11	0.00	0.00	0.10	0.010	0.10						
ETR	1.01	0.03	0.03	0.05	0.008	0.16						
	1.01	0.08	0.08	0.20	0.028	0.14						
ATR	0.33	0.05	0.15	0.55	0.010	0.02						
	0.33	0.13	0.39	0.55	0.067	0.12						
East Europe	1.08	0.08	0.07	0.10	0.031	0.31						
	1.08	0.12	0.11	0.20	0.068	0.34						
West Europe	0.12	0.08	0.67	0.10	0.048	0.48						
	0.12	0.05	0.42	0.10	0.060	0.60						
Sweden				0.02	0.005	0.25	1.1	0.02	0.018			
				0.05	0.043	0.86	3.2	0.12	0.037			
Germany				0.05	0.006	0.12	2.1	0.03	0.014			
				0.20	0.025	0.12	5.7	0.05	0.009			
Norway				0.02	0.017	0.85	1.4	0.04	0.029			
				0.05	0.025	0.50	6.8	0.18	0.026			
Greece				0.03	0.012	0.40	1.1	0.01	0.009			
UK							1.2	0.03	0.025			
							3.6	0.05	0.014			
							6.0	0.16	0.027			
Italy				0.10	0.032	0.32	3.6	0.11	0.031			
				0.30	0.062	0.21	7.2	0.66	0.092			
Yugoslavia				0.15	0.058	0.39	2.1	0.12	0.057			
North America				0.14	0.014	0.10	2.4	0.03	0.013			
							7.2	0.28	0.039			
							12.0	0.68	0.067			
Mean	**0.75**	**0.07**	***) 0.13**	**0.15**	**0.029**	**0.26**	**4.2**	**0.16**	**0.031**	**0.8**	**0.012**	**0.013**

*) without Western Europe

Table A7 Model calculation results of DDT assimilation and degradation, g/ha

	Measured accumulation	Model assimilation:			Degradation	Model error
		day	night	total		
Astrakhan	0.02	0.017	0.003	0.020	0.001	-0.001
	0.04	0.018	0.003	0.021	0.001	-0.020
Berezinsk	0.06	0.027	0.005	0.032	0.001	-0.029
	0.08	0.029	0.005	0.034	0.001	-0.047
Caucasian	0.05	0.082	0.015	0.097	0.003	0.044
	0.11	0.094	0.018	0.112	0.003	-0.001
Prioks_Terr	0.02	0.037	0.007	0.044	0.001	0.023
	0.03	0.044	0.008	0.052	0.002	0.020
Tsentr_Lesnoi	0.01	0.029	0.006	0.035	0.001	0.024
	0.04	0.034	0.006	0.040	0.001	-0.001
Barguzins	0.03	0.017	0.003	0.020	0.001	-0.011
	0.09	0.018	0.003	0.021	0.001	-0.070
Borovoe	0.03	0.026	0.005	0.031	0.001	0.000
	0.13	0.028	0.005	0.033	0.001	-0.098
Repetek	0.06	0.018	0.003	0.021	0.000	-0.039
Sary_Chelek	0.15	0.015	0.003	0.018	0.001	-0.133
	0.17	0.016	0.003	0.019	0.001	-0.152
Chatkalsk	0.06	0.020	0.004	0.024	0.001	-0.037
	0.07	0.022	0.004	0.026	0.000	-0.044
Abramov Glacier	0.01	0.006	0.001	0.007	0.001	-0.004
ETR	0.03	0.031	0.006	0.037	0.001	0.006
	0.08	0.039	0.007	0.046	0.001	-0.035
ATR	0.05	0.018	0.003	0.021	0.001	-0.030
	0.13	0.020	0.004	0.024	0.002	-0.108
East Europe	0.08	0.050	0.009	0.059	0.002	-0.023
	0.12	0.063	0.012	0.075	0.001	-0.046
West Europe	0.08	0.014	0.003	0.017	0.001	-0.064
	0.05	0.016	0.003	0.019	0.000	-0.031
Mean:	**0.07**	**0.030**	**0.006**	**0.036**	**0.001**	**-0.032**

Table A8 Calculation results of lindane assimilation, root uptake and degradation, g/ha

	Measured accumulation	Model assimilation: day	night	total	Root uptake	Degradation	Model error
Astrakhan	0.006	0.009	0.000	0.009	0.000	0.0011	0.002
	0.014	0.023	0.001	0.024	0.004	0.0034	0.011
Berezinsk	0.003	0.012	0.001	0.013	0.000	0.0016	0.008
	0.011	0.024	0.001	0.025	0.002	0.0032	0.013
Caucasian	0.014	0.017	0.001	0.018	0.001	0.0023	0.003
	0.039	0.051	0.003	0.054	0.012	0.0079	0.019
Prioks_Terr	0.011	0.030	0.002	0.032	0.003	0.0042	0.020
	0.065	0.045	0.002	0.047	0.007	0.0065	-0.018
Tsentr_Lesnoi	0.007	0.014	0.001	0.015	0.001	0.0019	0.007
	0.016	0.017	0.001	0.018	0.003	0.0025	0.003
Barguzinsk	0.018	0.016	0.001	0.017	0.005	0.0026	0.001
	0.010	0.007	0.000	0.007	0.002	0.0011	-0.002
Borovoe	0.008	0.019	0.001	0.020	0.001	0.0025	0.011
	0.020	0.040	0.002	0.042	0.003	0.0054	0.020
Repetek	0.034	0.022	0.001	0.023	0.004	0.0032	-0.010
Sary_Chelek	0.036	0.020	0.001	0.021	0.003	0.0029	-0.015
	0.084	0.067	0.003	0.070	0.006	0.0091	-0.017
Chatkalsk	0.032	0.021	0.001	0.022	0.001	0.0028	-0.012
	0.097	0.178	0.009	0.187	0.002	0.0227	0.069
Abramov Glacier	0.010	0.008	0.000	0.008	0.001	0.0011	-0.002
ETR	0.008	0.011	0.001	0.012	0.003	0.0018	0.005
	0.028	0.048	0.002	0.050	0.004	0.0065	0.020
ATR	0.010	0.007	0.000	0.007	0.001	0.0010	-0.003
	0.067	0.058	0.003	0.061	0.002	0.0076	-0.012
E.Europe	0.031	0.014	0.001	0.015	0.002	0.0020	-0.016
	0.068	0.031	0.002	0.033	0.004	0.0044	-0.035
Mean:	**0.029**	**0.031**	**0.002**	**0.032**	**0.003**	**0.0043**	**0.003**

Table A9 Calculation results of PCB-153 assimilation, g/ha

	Measured accumulation	Model assimilation:			Model error
		day	night	total	
Sweden	0.02	0.002	0.001	0.003	-0.017
	0.12	0.215	0.052	0.267	0.147
Germany	0.03	0.013	0.003	0.016	-0.014
	0.05	0.153	0.037	0.190	0.140
Norway	0.04	0.022	0.005	0.027	-0.013
	0.18	0.038	0.009	0.047	-0.133
Greece	0.01	0.002	0.000	0.002	-0.008
UK	0.03	0.001	0.000	0.001	-0.029
	0.05	0.046	0.011	0.057	0.007
	0.16	0.164	0.040	0.204	0.044
Italy	0.11	0.049	0.012	0.061	-0.049
	0.66	0.221	0.054	0.275	-0.385
Yugoslavia	0.12	0.057	0.014	0.071	-0.049
North America	0.03	0.131	0.032	0.163	0.133
	0.28	0.426	0.104	0.530	0.250
	0.68	0.822	0.200	1.022	0.342
Mean:	**0.16**	**0.148**	**0.036**	**0.184**	**0.023**

Table A10 Calculation results of B(a)P assimilation, g/ha

	Measured accumulation	Model assimilation:			Model error
		day	night	total	
Astrakhan	0.001	0.004	0.001	0.005	0.004
	0.002	0.004	0.001	0.005	0.003
Berezin	0.010	0.002	0.001	0.003	-0.007
	0.017	0.021	0.008	0.029	0.012
Caucasus	0.011	0.001	0.000	0.001	-0.010
	0.055	0.009	0.003	0.012	-0.043
Prioks_Terr	0.006	0.007	0.003	0.010	0.004
	0.013	0.024	0.009	0.033	0.020
Tsentr_Lesnoi	0.002	0.005	0.002	0.007	0.005
	0.027	0.005	0.002	0.007	-0.020
Barguzin	0.003	0.000	0.000	0.000	-0.003
	0.006	0.002	0.001	0.003	-0.003
Borovoe	0.004	0.007	0.003	0.010	0.006
	0.018	0.008	0.003	0.011	-0.007
Repetek	0.012	0.006	0.002	0.008	-0.004
Sary_Chelek	0.001	0.001	0.000	0.001	0.000
	0.012	0.002	0.001	0.003	-0.009
Mean:	**0.012**	**0.006**	**0.002**	**0.009**	**-0.003**

Chapter 3 Construction and description of climatological current fields in the upper ocean layer for transport models

A.A.Zelenko, Yu.D.Resnyansky, L.K.Erdman

Introduction

Transport in the atmosphere of many POPs, mercury and its compounds is not only the regional but global problem. Under global dispersion a significant part of pollutants enter oceans and seas via atmosphere. According to the assessment of [*Duce et al*., 1991] this value is to 80-99% for a number of POPs (e.g., polychlorinated biphenyls (PCB), hexachlorocyclohexanes (HCH), DDT or hexachlorobenzenes (HCB)). According to estimates of *S.Tanabe* [1986] the input of PCB to the environments amounts to more than 370 thous.tons out of which 230 thous.tons enter the water. Processes of contaminant spatial redistribution in the ocean are connected with both atmospheric fluxes and pollutant drift with currents. Within the framework of the Arctic Monitoring and Assessment Program (AMAP) a similar problem connected with contaminant transport by the polluted ice drift was considered.

The atmosphere/sea exchange can be realized due to the dry and wet deposition of the matter on and its re-emission from the sea to the atmosphere. The input takes place in both aerosol and gaseous forms, the re-emission, as a rule, is associated with the gasphase. For example, mercury enters the marine water on particles and as inorganic gaseous compounds and it re-emits mainly as gaseous elemental mercury.

The atmosphere/sea interaction is considered in a number of papers dedicated to pollution dispersion on the regional and global levels (for example, *GESAMP*, 1989; *Duce et al.*, 1991; *Duce*, 1997; *Fitzgerald and Mason*, 1996; *Cossa et al*., 1996; *Strand and Hov*, 1996; *Jacobs and van Pul*, 1996; *van Pul et al*., 1998; *van den Hout*, 1994). Calculation results and estimates given in these and other papers indicate that seas are not only receivers of pollutants depositing from the atmosphere, but also they are emitters. For example, in calculations carried out by *G.Petersen et al.* [1995] it is assumed that the ocean is a source of mercury input to the atmosphere *D.Cossa et al.* [1996] on the basis of balance calculations show that total input of mercury from the atmosphere to ocean margins is about 400 t/y and from these regions to the atmosphere - about 500 t/y. A number of authors [*Tatsukawa et al*., 1990; *Bidleman et al*., 1990] indicate that during a long period of time the ocean is a reservoir not only of PCB input but also of its emission. *T.F.Bidleman et al.* [1995] point out that northern seas become re-emission source of lindane due to the reduction of atmospheric concentrations.

Oceanic currents play a significant role in the processes of atmosphere/sea POPs exchange. In generalized form they are taken into account in global block models (e.g. [*Strand and Hov*, 1996]). In paper [*Jacobs and van Pul*, 1996] it is indicated that the calculated re-emission of lindane from the sea calculated by the authors appeared to be overestimated since the effect of sea current transporting and mixing lindane in the horizontal direction was not taken into account. In paper by *W.Fitzgerald and R.Mason* [1996] ocean currents along with air flows explain the atmosphere/ocean interaction in temperate and tropical latitudes (see the scheme taken from this paper).

MSC-E has started to evaluate the sea current influence on the atmosphere/ocean exchange processes. Present work is devoted to a review of the basic features of surface sea currents and vertical redistribution in sea-water within the EMEP grid.

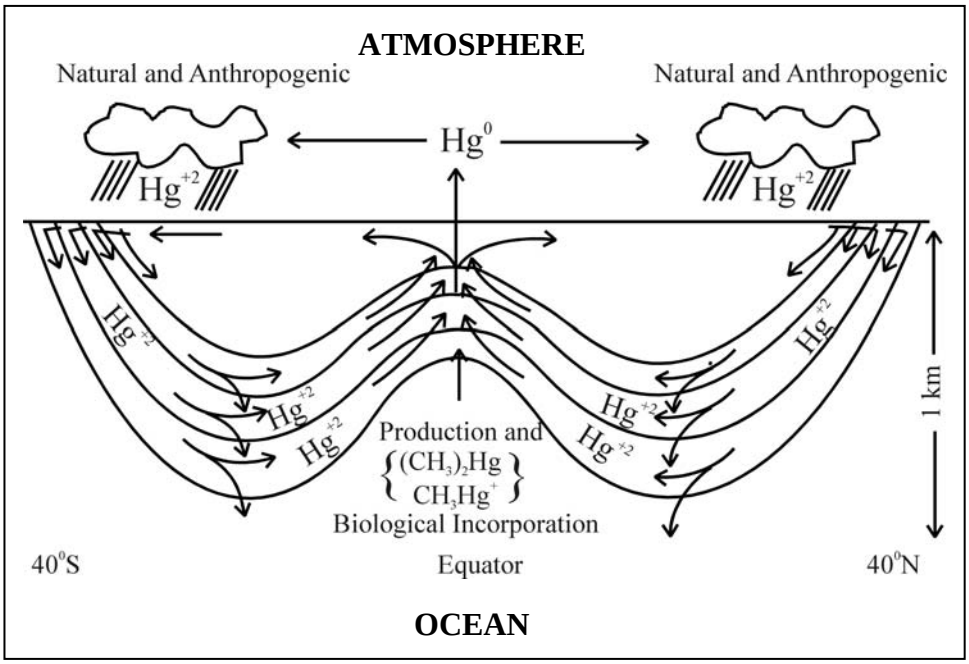

The scheme was taken from *W.F.Fitzgerald and R.P.Mason* [1996].

1 General information on sea currents

Ocean (sea) currents are a combination of periodic and aperiodic movements of water particles induced by internal and external forces. Depending on the relationship between basic forces determining the balance in dynamic equations the following types of movements [*Neumann*, 1973; *Lacombe,* 1974; *Zhukov*, 1976] can be distinguished: steady/unsteady, barotropic/barocline, geostrophic, drift, cyclostrophic, inertial, tidal, hydraulic, compensational etc. Depending on temporal scales unsteady processes in the ocean are classified into small-scale, meso-scale ones, processes of synoptic variability, seasonal, interannual, intracentennial and intercentennial variations [*Monin et al.,* 1974].

Small-scale phenomena (with a period from fractions of seconds to tens of minutes) are surface and internal waves, turbulence and processes of evolution of the vertical microstructure. Turbulence is a principal mechanism of the vertical mixing in the ocean and in particular of its exchange of momentum, heat and admixtures with the atmosphere leading to large-scale variations of the ocean. Turbulence is most intensive in the upper mixed layer with depth of several tens of metres.

Mesoscale phenomena (with the periods of hours to days) are tidal and inertial fluctuations arising under the effect of gravitational forces of the Moon and the Sun and inertial forces induced by the rotational movement of the planet.

Synoptic variability (with periods of several days to several months) is an aperiodic formation of eddies of the scale of about 100 km (to a considerable extent similar to atmospheric cyclones and anticyclones but with appreciably longer life-time and much

slower movement). These eddies are formed due to the accumulated atmospheric effects and due to hydrodynamic instability of large-scale ocean currents.

Seasonal variations (annual period and its harmonics) are obviously caused by annual variations the solar radiation influx and by a sequence of subsequent changes in the ocean-atmosphere system.

In the formation of interannual variability exemplified by auto-oscillations of the northern part of the Gulf Stream with the period of about 3.5 years and the El Nino - Southern oscillation phenomenon in the tropical part of the Pacific Ocean etc., a noticeable role obviously plays the movement of thermal anomalies along giant ocean gyres bending over by waters during several years.

Intracentennial and intercentennial variations (with decades and centenary periods) are referred to climatic variations determined by the dynamics of the Earth climate system.

From the above said it follows that a strictly steady motion in the ocean is impossible since waters are continuously affected by various unstationary disturbances. For practical purposes, however, instantaneous states of the World Ocean can be conveniently presented as a sum of mean multiannual states (a quasi-steady part which varies with a time period of several decades and more may be called climatic) and deviations from them caused by short-period unsteady processes.

Instantaneous states of the ocean are more similar to its mean multi-annual state than in the atmosphere. In other words, the total relative intensity of short-term processes in the ocean is lower than in the atmosphere, because the inertia of the ocean is higher. In fact, instantaneous states of the atmosphere reflected, for example, on daily synoptic charts have little to do with the mean multi-annual pattern of its circulation containing several languid cells or «wheels» of circulation in meridianal cross-sections. The ocean is characterized by the same system of basic currents with relatively slight changes in the geographical distribution and intensity. Therefore the quasi-steady part of the World Ocean state depicted on maps of ocean atlases gives a fairly good representation of instantaneous states of its global circulation. This state can be considered as a background against which short-term unsteady processes are developed.

In spite of the similarity of a general pattern of instantaneous and quasi-steady processes within the scale of ocean basins, the magnitude of unsteady processes in specific regions can reach high values exceeding the quasi-steady part. First of all it refers to drift currents in the upper ocean layer with depth of several tens of metres and to synoptic eddies penetrating to depths of hundreds and thousands of metres.

2 Methods of determination of sea currents

Sea currents can be determined by two ways:

1) direct measurements by various instruments;
2) indirect calculation methods which are reduced to calculations of current characteristics using other known (measured) hydrometeorological parameters.

2.1 Direct methods

Measurement of currents in the open ocean is a rather complicated and expensive thing. The application of equipment hung up to a floating platform is connected with great expenditures of devices manufacture and installation (moored buoys) and maintenance of these platforms (ships). The task is also complicated by the fact that these platforms are not fixed. They are moved by wind, waves and by the measured currents themselves. Buoys moored by long, elastic lines are subject to the same but somewhat restricted movements, which are transmitted via the line to current meters introducing distortions into their records.

Nowadays measurements of currents with the help of Lagrangian type devices - surface drifting buoys and submerged neutral buoyancy floats are receiving increasing recognition. Spatial location of these devices in subsequent moments of time is fixed by space navigation systems and transmitted to centers of information collection by telecommunication channels in the on-line regime. Nevertheless the number of such devices still remains insufficient for the assessment of the instantaneous state of the World Ocean waters. Detailed measurements are available only for limited basins and for limited intervals of time during special experiments and expeditions. The best known examples are experiments related to investigation of synoptic eddies in the Atlantic Ocean (Poligon-70, MODE, Polimode; see [*Investigations of synoptic variability of the ocean*, 1977]), complex observations under TOGA program in the tropical Pacific [*WMO/TD*, 1995] and a large-scale experiment aimed at the investigations of the World Ocean circulation (WOCE) which is under way.

A prototype of modern Lagrangian means of current measurements is the eldest and simple method used since the middle of the XIX century and based on the processing of navigation records in log-books. The current is determined from the difference between ship location determined by the dead reckoning and astronomic observations. In spite of the fact that data on the ship drift obtained by this way are not quite precise and partially they depend on a direct shift of ships by wind, but a great number of observations can provide fail good estimate of a general pattern of the averaged flow.

The majority of atlases of surface currents published until recent years to a considerable extent are compiled on the basis of this method [*Marine Atlas*, 1953].

2.2 Indirect methods

Insufficient measurement data stimulated the development of indirect or computational methods of sea current determination. These methods are reduced to the development and application of one or another model of ocean currents. The range of models is very broad, from the simplest empirical relationships relating, for example, the surface drift current to the wind speed, to rather sophisticated mathematical models based on a full set of equations for dynamics and thermodynamics of the ocean.

The intermediate place is occupied by simplified theoretical models applied in specific cases. These models made the ground for the development of classical dynamic oceanography as an independent branch of science at the beginning of the XX century [*Neumann*, 1973; *Lacombe*, 1974; *Zhukov*, 1976]. Among such models the so-called dynamic method of current calculations is distinguished. It appeared to be rather good for the description of a general pattern of the ocean circulation.

2.3 Dynamic method of current calculations

The dynamic method introduced in meteorology by Bjerknes in 1989 was applied to oceanography by Sandstrom and Helland-Hansen [*Sandstrom and Helland-Hansen*, 1903]. This method is based on the assumption that the motion is quasi-steady and acceleration balance for horizontal components of the motion is determined by the pressure gradient and Coriolis forces:

$$fu + \frac{m}{\rho}\frac{\partial p}{\partial y} = 0, \qquad fv - \frac{m}{\rho}\frac{\partial p}{\partial x} = 0, \tag{1}$$

and along the vertical hydrostatic relationship is fulfilled,

$$\partial p / \partial z - g\rho = 0 . \tag{2}$$

Here u and v are the horizontal components of water motion velocity vector along (x and y) axes respectively; x and y are the axes of Cartesian co-ordinate system in the plain of polar stareographic projection; z is the vertical co-ordinate directed downwards; p is the pressure; ρ is the sea water density; $m=(1+\sin\varphi_1)/(1+\sin\varphi)$ is the scale multiplier for the polar stereoraphic projection; φ is the geographycal latitude; φ_1 is the latitude of the projection cross-section, $f = 2\cdot\omega\cdot\sin\varphi$ is the Coriolis parameter, ω is the angular velocity of the Earth rotation.

Like in meteorology, the current occurred under these assumptions is called geostrophic. The assumptions made are valid for comparatively slow motions (Rosby number $R_0=U/fL<<1$, U is the characteristic velocity, L is the characteristic length scale) when external forces (pressure gradient and Coriolis forces are internal ones) and of friction forces are absent or relatively small. As scale estimates show these conditions are fulfilled for large-scale ocean motions outside the boundary layers (coastal, near bottom, surface) where friction is of a considerable importance. Hence, in particular, it follows that the dynamic method is inapplicable to calculations of pure wind component of the current velocity and for shallow regions.

Introducing geopotential height (in oceanography the term «dynamic height» is also used) of the isobaric surface p:

$$D = \int_{p_0}^{p} \alpha dp , \tag{3}$$

eq.(1) allowing for (2) can be rewritten in the following way

$$u = -\frac{m}{f}\frac{\partial D}{\partial y}, \qquad v = \frac{m}{f}\frac{\partial D}{\partial x}, \tag{4}$$

where $\alpha=1/\rho$ is the specific volume of the ocean water.

From (4) it follows that the calculation of current by the dynamic method is reduced to the determination of slopes $\partial D/\partial x$, $\partial D/\partial y$ of the corresponding isobaric surface. Dynamic heights D, according to (3), are calculated from density (specific volume $\alpha=1/\rho$) distribution in the layer from p_0 to p. In its turn density ρ depends on temperature T, salinity S and pressure p in accordance with the equation of state for the sea water.

$$\rho = \rho(T, S, p) \tag{5}$$

Therefore for the calculation of currents by the dynamic method it is necessary to know distributions of temperature and salinity as functions of pressure. Since specific volume of water α varies within a narrow range then there is an unambiguous and sufficiently accurate (within 1%) correspondence between pressure and geometric depth which hydrological measurements and summarized climatological data sets are referred to.

It is important to note that current velocities obtained by formula (4) allowing for (3) are not absolute values but relative velocities on isobaric surface p relative to isobaric surface p_0. Absolute values can be obtained only if we have direct or indirect information on currents at level p_0.

This fact raises the problem of selecting the so-called «zero surface», i.e. surface at which the horizontal pressure gradient and geostrophic currents vanish. This is a purely oceanographic problem which has no meteorological analogue, since the network of surface and upper-air observations allow to obtain absolute pressure near the ground surface and at different heights in the atmosphere.

Known methods of the estimation of «zero surface» depth are summarized in [*Neumann*, 1973; *Lacombe*, 1974; *Zhukov*, 1976]. All these methods are of an approximate character and as a consequence the currents determined by the dynamic method should be considered to a considerable extent as generalized estimates of a qualitative pattern of oceanic currents. According to Defant [*Zhukov*, 1976] in the North Atlantic «zero surface» lies at depths from 500 to 2000 dbar (from 500 to 2000 geometric metres). The characteristic value is 1000 dbar for the whole basin.

3 Source data and procedure for calculation of climatological currents within the EMEP domain using the dynamic method

3.1 Computational domain and the EMEP grid

A rectangular region in the plain of polar stereographic projection (cross-section at 60^0N) which corners have the following geographic co-ordinates: (λ=324.32°, φ=40.65°), (λ=13.00°, φ=24.08°), (λ=229.87°, φ=86.59°), (λ=58.53°, φ=40.74°) was considered to be the EMEP domain. The y axis is parallel to meridian 328^o. The grid with gridsize 50 km contains 117 points along x axis and 111 points along y axis. The pole coincides with the grid point having indices (8,110).

The considered domain covers the north-eastern part of the Atlantic ocean, North, Norwegian, Greenland, Barents Seas and a part of the Northern polar basin. The inner Seas (Baltic, White, Black, Caspian Seas) also located within this region were excluded from the subsequent consideration, since the source of hydrological data used contains insufficient information on these seas, and the conditions of the dynamic method applicability are not fully satisfied for these basins.

3.2 Source of hydrographic data

Initial data on water temperature and salinity were taken from the most complete modern climatological summary for hydrography of the World Ocean - electronic atlas WOA-94 [*Levitus and Boyer,* 1994; *Levitus et al.,* 1994]. The atlas was compiled at the National Oceanographic Data Center (USA) under the supervision of *S.Levitus*. The entire electronic

version contains nine CD-ROMs with data on climatology distributions of water temperature and salinity for each month of the year related to grid points of a regular geographical grid 1^0x1^0 at standard levels: 0, 10, 20, 30, 50, 75, 100, 125, 150, 200, 250, 300. 400, 500, 600, 700, 800, 900, 1000 m. For deeper levels there are only seasonal distributions which were not used in subsequent calculations.

The data analysis showed that climatological temperature distributions presented in the atlas had a number of inaccuracies appearing in some regions as great deviation from data of other sources. Therefore a search of refined data in the Internet has been undertaken. Thus initial data sets were corrected and used in calculations presented below.

3.3 Transformation of data and calculations of geostrophic currents

The calculation of geostrophic currents in the EMEP domain was made in the following sequence.

1. Data sets of temperature and salinity given at the points of a geographical grid 1^0x1^0 were reinterpolated to 50x50 km EMEP grid points with regards to the irregularity of the oceanic part of the grid. Nodes falling on land and inner water basins excluded from the consideration were filled with a no data indicator.
2. Grid fields of temperature and salinity obtained at the first step were used as initial data for the determination of dynamic height differences between standard levels. For the calculation of sea water density the equation of state suggested by the Joint panel on oceanographic tables and standards [*UNESCO,* 1981] was used. The results of computation were recorded in the intermediate file.
3. On the basis of data on dynamic height differences geostrophic currents at the ocean surface relative to 1000 dbar level were calculated using finite-difference analogue of formulas (4). As it was mentioned above this level is characteristic of the "zero surface " depth in the North Atlantic. In places where the depth was less than 1000 m the nearest to the bottom standard level was taken as the reference level. Certainly it is rather approximate method and resulted estimates of geostrophic currents in such places (for example, the North and Barents Seas, Farero-Iceland and other thresholds dividing sea basins) should be considered only as approximate ones. However, within the framework of the model accepted for the determination of currents there is no unambiguous method for the transition from relative velocities to absolute ones.
4. The calculated current velocities were recorded to output files together with data on sea surface temperatures. This file with the obtained current velocities and temperature is intended for subsequent calculations of the pollution transport.
5. At the final step the output numerical data sets were used for plotting of climatological charts of the surface geostrophic velocities and surface temperature fields for each of 12 months. These charts are discussed in the next section.

3.4 Files of numerical values of current velocities and sea surface temperatures (SST)

The obtained fields of geostrophic current velocities and SST have been recorded in unformatted (binary) file, which contains only data (without additional information on the

length of the record and the like). In Fortran a description of such a file should contain the option form='binary'.

The file structure and the ways of referring to it are illustrated by two fragments of Fortran-programs for data reading.

1) Sequential reading of data for 12 months:

```
c    Init of the fragment 1
     REAL T(117,111), U(117,111), V(117,111)
     OPEN(10, FILE='OCEAN.BIN', FORM='BINARY')
     DO MON=1,12
       READ (10) T,U,V  ! reading of temperature and current
                        ! velocity components on the EMEP! grid  month by month
     ENDDO
c    End of the fragment 1
```

2) Arbitrary access to data on any month

```
c    Init of the fragment 2
     REAL T(117,111), U(117,111), V(117,111)
     OPEN(10, FILE='OCEAN.BIN', FORM='BINARY',
    *        ACCESS='DIRECT',  RECL=117*111*3*4)
c
     IREC = 12                    ! reading of SST and current velocity
     READ (10,REC=IREC) T,U,V  ! components for December
     ...
c    End of the fragment 2
```

Data in the arrays T,U,V sets are ordered with respect to the first index from the left to the right and with respect to the second one - from the bottom to the top. For the corner grid points the temperature data set as an example it looks like the following is used:

T(001,001) - lower left corner of the domain,

T(117,001) - lower right corner of the domain,

T(001,111) - upper left corner of the domain,

T(117,111) - upper right corner of the domain.

“No data” indicator is – 99.999.

4 Basic peculiarities of climatological currents and sea surface temperature in the EMEP domain

The obtained climatological geostrophic currents for January and July are shown in Figures 1 and 2 together with surface temperature fields.

Vectors of the calculated currents are denoted by arrows oriented along the current direction (i.e. to the direction of their flow, contrary to traditional for meteorology agreement on wind - from where it blows). To make it more descriptive arrows are plotted only in each third node along both axes. Arrow lengths are proportional to velocity module $|\mathbf{u}|$. SST field, which is a scalar variable, is presented with the use of the gradation scale.

There are the following basic currents in the considered region:

1) a branch the North Atlantic current system directed from the south-west to the north-east to the northern extremity of Great Britain;
2) to the north of Great Britain Island this branch is transferred to the Norwegian current going along the Scandinavian coast;
3) its continuation to the north of North Cape, the Norwegian current changes to the North Cape current inflowing into the Barents Sea;
4) another branch of the Norwegian current is the Spitsbergen current directed almost along the meridian to Spitsbergen Island;
5) the North Cape current in combination with other less intensive streams forms a cyclonic gyre in the Barents Sea; this is clearly seen in the chart of stream lines presented in Figure 3 and corresponding to geostrophic currents for February;
6) in a similar way, the Norwegian and the Spitsbergen currents in combination with adjacent to Greenland and going to the south East-Greenland current form the cyclonic gyre in the basins of Greenland and Norwegian Seas;
7) in the surface layer of the Mediterranean Sea predominant currents are directed to the east; these streams are compensated by the subsurface outflow of salt Mediterranean water in the opposite direction.

According to data [*Marine Atlas,* 1953] mean current velocities in the considered region lay within the range up to 25 cm/s. Typical values of calculated geostrophic currents are 3-6 cm/s. There is a ground to believe that these velocities are underestimated as much as about 2-3 times for two reasons. First, accepted reference water level 1000 dbar is characteristic of the North Atlantic on the whole. In the considered region this level as judged from the map of "zero surface " according to Defant [*Zhukov*, 1976] is closer to 1500 dbar. Secondly, input hydrographic data are essentially smoothed climatological fields, that leads to a decrease of horizontal gradients and calculated velocities.

Nevertheless calculations reproduce a realistic general pattern of currents. On the charts of vector fields (Figures 1,2) and of stream lines (Figure 3), presented here as an example, one can find all main elements of the oceanic circulation mentioned above.

Its seasonal variations are illustrated in Figure 4 showing vector differences between winter (January) and summer (July) currents. These differences indicate an increase of the final branch of the North Atlantic current near Great Britain Island from winter to summer, a

decrease of the East Greenland current and some increase of water flow into the Mediterranean Sea. In other places seasonal variations are less pronounced and have no regular patterns.

The most noticeable peculiarity of SST field resides in predominating orientation of isothermals to the north of 20^0N from the south-west to the north-east, i.e. in the direction of main branches of ocean currents mentioned above. To the south of 20^0N the isotherms orientation is nearly zonal. The Arctic basin, which is covered by multiyear ice, has homogeneous water with the temperature close to that of freezing.

The amplitude of SST variations (the lower part of Figure 4) changes from zero (in near polar regions) to 11-12^0C near the ocean coast and in the Mediterranean Sea. Even greater seasonal variations are observed in the Baltic Sea.

5 Assessments of passive pollutant transport between the upper mixed layer and lower ocean layers

The vertical transport in the ocean is realized by two main mechanisms: 1) by ordered vertical motions connected with ocean currents; 2) as a result of mixing produced by small-scale turbulent diffusion.

5.1 Ordered vertical motions

Vertical motions w are very weak in the ocean and cannot be measured directly. Indirect methods are based on these or those models. For the following discussion of w estimates within the framework of some of these models it is more convenient to use the spherical co-ordinate system (λ, φ, z), since it naturally reflects effects of the Earth sphericity being important in some cases.

Vertical velocities w can be calculated from continuity equation:

$$(1/ (a \cos \varphi)) \partial u/\partial \lambda + (1/ (a \cos \varphi)) \partial (v \cos \varphi) /\partial \varphi + \partial w/\partial z = 0, \quad (6)$$

where (u,v) are horizontal velocity components in the spherical co-ordinate system, w is the vertical component of velocity along z axis directed downwards, a is the Earth radius.

Integration of (6) over by the vertical between $z=z_1$ and $z=z_2$ yields:

$$w(z_2) - w(z_1) = - \int_{z_1}^{z_2} [(1/(a \cos\varphi))\partial u / \partial \lambda + (1/(a \cos \varphi))\partial (v \cos \varphi) / \partial \varphi] dz \quad (7)$$

Thus the vertical velocity is determined by the divergence of horizontal movements integrated over depth.

5.2. Vertical motions in geostrophic currents

Geostrophic currents are determined by formulas (analogue of (1) in the spherical system of co-ordinates):

$$u = -\frac{1}{\rho f} \frac{\partial p}{a \partial \varphi}, \qquad v = \frac{1}{\rho f} \frac{\partial p}{a \cos \varphi \partial \lambda}, \quad (8)$$

Substituting (8) into (7) one obtains:

$$w(z_2) - w(z_1) = \frac{\beta}{f}\int_{z_1}^{z_2} \frac{1}{\rho f}\frac{\partial p}{a\cos\varphi \partial\lambda} dz = \frac{\beta}{f}\int_{z_1}^{z_2} v dz \qquad (9)$$

where $\beta = (1/a)\partial f / \partial\varphi = (2\omega/a)\cos\varphi$ is the latitudinal variations of Coriolis parameter, ω =7.29 10^{-5} is the angular velocity of the Earth rotation.

Thus geostrophic currents are almost non-divergent. Weak divergence arises from the Earth sphericity due to which the Coriolis parameter depends on latitude. In middle latitudes f~10^{-4}s^{-1}, β~10^{-11} m^{-1}s^{-1} and the characteristic value of the vertical velocity difference over the distance of about 100 m with v=0.1 m s^{-1} is 10^{-6} m s^{-1}. This seemingly negligible value (about 30 m/year) nevertheless can be essential for the pollution transport from the upper ocean layer. The thing is that in large-scale ocean gyres such as subtropical anticyclonic gyre or subpolar cyclonic gyre the sign of v and consequently of w remains unchanged for a long time. Vertical movements of water particles in spite of small velocity values have a cumulative effect during long time interval and determine the admixture transport either from the underlying layers where v>0 or from the upper layer to deep ones at where v<0.

5.2.1 Vertical motions in drift currents (Ekman pumping)

Classical Ekman model of drift currents is based on the assumption that the acceleration balance in the upper ocean layers is determined by friction and Coriolis forces. In the steady case the corresponding equations are written in the following form:

$$-fv = -\frac{1}{\rho}\frac{\partial\tau_\lambda}{\partial z}, \qquad fu = -\frac{1}{\rho}\frac{\partial\tau_\varphi}{\partial z} \qquad (10)$$

where $((\tau_\lambda, \tau_\varphi))$ are the components of the tangential stress vector τ in water resulted from small-scale turbulent mixing.

In order to calculate the current vertical structure (u,v) from (10) it is necessary to express $(\tau_\lambda, \tau_\varphi)$ via currents themselves (u,v). An ordinary hypothesis is $\tau_\lambda = -k_z\rho\partial u/\partial z$, $\tau_\varphi = -k_z\rho\partial v/\partial z$, where k_z is the coefficient of vertical turbulent mixing. However, for the evaluation of vertical motions connected with drift currents it is sufficient to note that at the water surface z=0: $\tau_\lambda = \tau_{\lambda a}$, $\tau_\varphi = \tau_{\varphi a}$ ($\tau_{\lambda a}$, $\tau_{\varphi a}$ are the components of wind tangential stress at the water surface) and at the lower boundary of Ekman layer $z=z_e$ (in middle latitudes several tens of metres) the stresses vanish: τ_λ=0, τ_φ=0. Then substituting expressions for (u,v) from (10) to continuity equation (7) where z_1=0, $z_2=z_e$, at a reasonable assumption, $w(0)$ = 0, one obtains:

$$w(z_e) = -rot_z(\frac{\tau_a}{\rho f}), \qquad (11)$$

i.e. vertical velocity at the lower boundary of Ekman layer (the layer of drift currents) is proportional to the vertical component of tangential wind stress curl.

Characteristic value of $|\boldsymbol{\tau}_a|$ at wind speed 10 m/s is 0.2 H/m^2; at strong wind of about 20 m/s $|\boldsymbol{\tau}_a|$ ~ 0.8 H/m^2. For the cyclone with diameter of 1000 km with such a wind we have $|rot_z(\tau_a/(\rho f))| = |w(z_e)|$=1.5 10^{-5} m/s. This value (about 1,3 m/day) is more than an order of magnitude higher than vertical motions in geostrophic currents. In zones with strong wind

vorticity the Ekman pumping mechanism can be determining for the admixtures transport from the upper ocean layer.

5.2.2 Vertical motions in coastal zones

Coastal upwelling (downwelling) zones are produced as a result of interaction of currents with coasts [*Lacombe*, 1974; *Gill*, 1986]. Due to continuation of water medium the horizontal current running towards the coast produces descending motions (downwelling), and the forces driving water back from the coast give rise to ascending motions (upwelling). Similar phenomena can arise not only near coasts but also at the boundaries which cannot be crossed by the water for any of several reasons at boundaries between the equatorial current and counter current.

The upwelling intensity in a specific region is proportional to variations of Ekman flow. In coastal regions this flow varies from zero to values characteristic for the open ocean at the distance of about Rossby deformation radius, i.e. about 30 km [*Gill*, 1986]. Similar variations of Ekman flows in the open ocean are observed only on synoptic scales, i.e. 1000-3000 km. Hence the upwelling intensity in coastal regions should be 30-100 times higher than in the open ocean. According to some estimates [*Gill*, 1986] the upwelling velocity can reach 5 m/day.

Main upwelling zones are observed near the eastern boundaries of the ocean. The information about downwelling zones is less certain. By analogy, however, it may be supposed that descending motions in coastal zones reach the same intensity as ascending ones.

5.3 Turbulent diffusion

Small-scale turbulence responsible for mixing of all substances, including admixtures, is generated in the upper layer as a result of surface waves breaking, velocity vertical shear in drift currents and density convection due to cooling of the surface water or increasing salinity. As a result the Upper Mixed Layer (UML) is observed, within which vertical distributions of temperature, salinity and other elements are almost homogeneous [*Zilitinkevich et al.*, 1978]. In middle latitudes the UML depth has a pronounced seasonal variation - from 10-20 m in summer to 200 m and more in winter.

The turbulent diffusion coefficient k_z in the UML is about 10^{-3}-10^{-2} m^2/s. Mean square displacement of pollution particles increases with time following the law $(2k_z t)^{1/2}$ [*Monin et al.*, 1974].

Under the UML there is a discontinuity layer with the highest vertical gradients of density. In this layer vertical diffusion coefficient is essentially decreased (by 1-2 orders of magnitude compared with the UML) due to restricting limiting effect of density stratification.

Below the discontinuity layer, in seasonal (or upper) thermocline, on the average monotonous density increase with the depth is observed; however, in specific cases one or several discontinuities can take place here. Against their background a complex microstructure is observed and as a result the thermocline appeared to be composed from numerous quasi-homogeneous layers separated by thinner layers with jumps in density and weak or vanishing turbulence.

Neighboring layers often have different turbidity and salinity, which points out to their independent ways of evolution during appreciable time periods and to rather slow exchange via intermediate layers. It is confirmed by observations of Isaacs and Folson [*Formation, structure and fluctuations...,* 1971] who found that radioactive fallout deposited in the thermocline was kept within a discrete layers about 7 m depth during many days.

The most effective mechanism of pollutant exchange between the UML and underlying layers is entrainment - trapping of lower weakly turbulized water by the mixed layer during its deepening. Vertical flux of substance F_C, which concentration in the UML is C_m and in the lower layer C_l accounts for:

$$F_C = (C_m - C_l)\partial h / \partial t \tag{12}$$

where h is the mixed layer depth varying with time t.

Under the conditions of storm winds the UML deepening rate reaches 10-15 m/day. The alteration of ascending and desending motions of the UML lower boundary can cause a very intensive exchange of pollutants between the UML and lower layers. In order to make a quantitative description of this process it is necessary however to develop models similar to those describing the UML [*Zilitinkevich et al.*, 1978].

References

Bidleman T.F., Jantunen L.M., Falconer R.L. and Barrie L.A. [1995] Decline of hexachlorocyclohexane in the arctic atmosphere and reversal of air-sea gas exchange. Geophys.Res.Lett., v.22, pp.219-222.

Bidleman T.F., Patton G.W., Hinckley D.A., Walla M.D., Cotham W.E. and Hargrave B.T. [1990] Chlorinated pesticides and polychlorinated biphenyls in the atmosphere of the Canadian arctic. Long-Range Transport of Pesticides. D.A.Kurz ed., Lewis Publishers, Inc., Chelsea, MI, pp.347-372.

Cossa D., Coquery M., Gobeil C. And Martin J.-M. [1996] Mercury Fluxes at the Ocean Margins. In: Global and Regional Mercury Cycles: Sources, Fluxes and Mass Balances. Ed. by W.Baeyens, R.Ebinghaus and O.Vasiliev. NATO ASI Series, 2. Environment, v.21. Kluwer Academic Publ., Dordrecht, pp.229-248.

Duce R.A. [1997] Atmospheric Input of Pollution to the Oceans. Marine Meteorology and Related Oceanographic Activities, v.39.

Duce R.A., Liss P.S., Merrill J.T. et al. [1991] The atmospheric input of trace species to the World Ocean. Global Biogeochem. Cycles, v.5, pp.193-259.

Fitzgerald W.F. and Mason R.P. [1996] The Global Mercury Cycle: Oceanic and Anthropogenic Aspects. In: Global and Regional Mercury Cycles: Sources, Fluxes and Mass Balances. Ed. By W.Baeyens, R.Ebinghaus and O.Vasiliev. NATO ASI Series, 2. Environment, v.21. Kluwer Academic Publ., Dordrecht, 85-108.

Formation, structure and Fluctuations of upper thermocline in the ocean [1971] Collection of articles, translation from English, L., Hydrometeoizdat.

GESAMP [1989] The atmospheric Input of Trace Species to the World Ocean. Rep.Stud. GESAMP, v.38, pp.1-111. World Meteorological Organization, Geneva, Switzerland.

Gill A. [1986] Atmosphere-Ocean Dynamics. Translation from English. T.2, M., Mir.

van den Hout K.D. (ed.) [1994] The Impact of Atmospheric Deposition of Non-Acidifying Pollutants on the Quality of European Forest Soils and the North Sea. Main report of the ESQUAD project. IMW-TNO report 93/329, Delft, The Netherlands, p.121.

Investigations of oceanic synoptic variability in the ocean [1977] Materials of the USSR-USA Institute POLIMODE (Jalta, 1976), Sevastopol, Published by Marine Hydrophysical Institute of the Ukrainian SSR Academy of Sciences.

Jacobs C.M.J. and van Pul W.A.J. [1996] Long-range atmospheric transport of persistent organic pollutants, I: Description of surface-Atmosphere exchange modules and implementation in EUROS. National Institute of Public Health and the Environment, Bilthoven, The Netherlands. Report No.722401013.

Lacombe H. [1974] Physical Oceanography. Translation from French, M., Mir.

Levitus S. and Boyer T.P. [1994] World Ocean Atlas 1994 v.4: Temperature. NOAA Atlas NESDIS 4.

Levitus S., Burgett R. and Boyer T.P. [1994] World Ocean Atlas 1994 Vol.3: Salinity. NOAA Atlas NESDIS 3.

Marine Atlas [1953] v.II. Physical-Geographycal, ed. By I.S.Isakov, V.V.Shuleikin, L.A.Demin. Published NAVY Headquarters of the USSR Ministry of Defence.

Monin A.S., Kamenkovich V.M., Kort V.G. [1974] Variability of the World Ocean, L., Hydrometeoizdat.

Neumann G. [1973] Ocean currents. Translation from English, Hydrometeoizdat.

Petersen G., Iverfeldt A. and Munthe J. [1995] Atmospheric mercury species over central and northern Europe. Model calculations and comparison with observations from the nordic air and precipitation network for 1987 and 1988. Atmos.Environ., v.29, pp.47-67.

van Pul W.A.J., Nijenhuis W.A.S. and de Leeuw F.A.A.M. [1998] Deposition of heavy metals to the Convention waters of OSPARCOM. National Institute of Public Health and the Environment, Bilthoven, The Netherlands. Report No.722401016.

Sandstrom J.W. and Helland-Hansen B. [1903] Uber die Berechnung von Meeresstromungen. Rep. Norv. Fish. Marine Invest., v.2, No 4. Bergen.

Strand A. and Hov O. [1996] A model Strategy for the Simulation of Chlorinated Hydrocarbon Distribution in the Global Environment. Water, Air and Soil Pollution, v.86, pp.283-316.

Tanabe S. [1986] Distribution, behaviour and fate of PCBs in the marine environment of Oceanological Society of Japan, v.41, No.5 (In Japan).

Tatsukawa R., Yamaguchi Y., Kawano M., Kannan N. And Tanabe S. [1990] Global Monitoring of Organochlorine Insecticides-And 11-year Case Study (1975-1985) of HCHs and DDTs in the Open Ocean Atmosphere and Hydrosphere. Long-Range Transpor of Pesticides, Chapter 10, Lewis Publishers, Chelsea. MI.

UNESCO [1981] Tenth report of the joint panel on oceanographic tables and standards. UNESCO Tech. Pap. Marine Sci. No 36, UNESCO, Paris.

WMO/TD No.717 [1995] Proceedings of the International Scientific Conference on the Tropical Ocean Global Atmosphere (TOGA) Programme (2-7 April 1995, Melbourne, Australia) WCRP-91, WMO/TD No. 717, Dec. 1995.

Zhukov L.A. [1976] General oceanology, L., Hydrometeoizdat.

Zilitinkevich S.S., Resnyansky Yu.D., Chalikov D.V. [1978] Theoretical modelling of the upper ocean layer. In book: Science and Technology Results. Mechanics of liquid and gas. T.12, M., Published by All-Union Institute of Scientific and Technological Information.

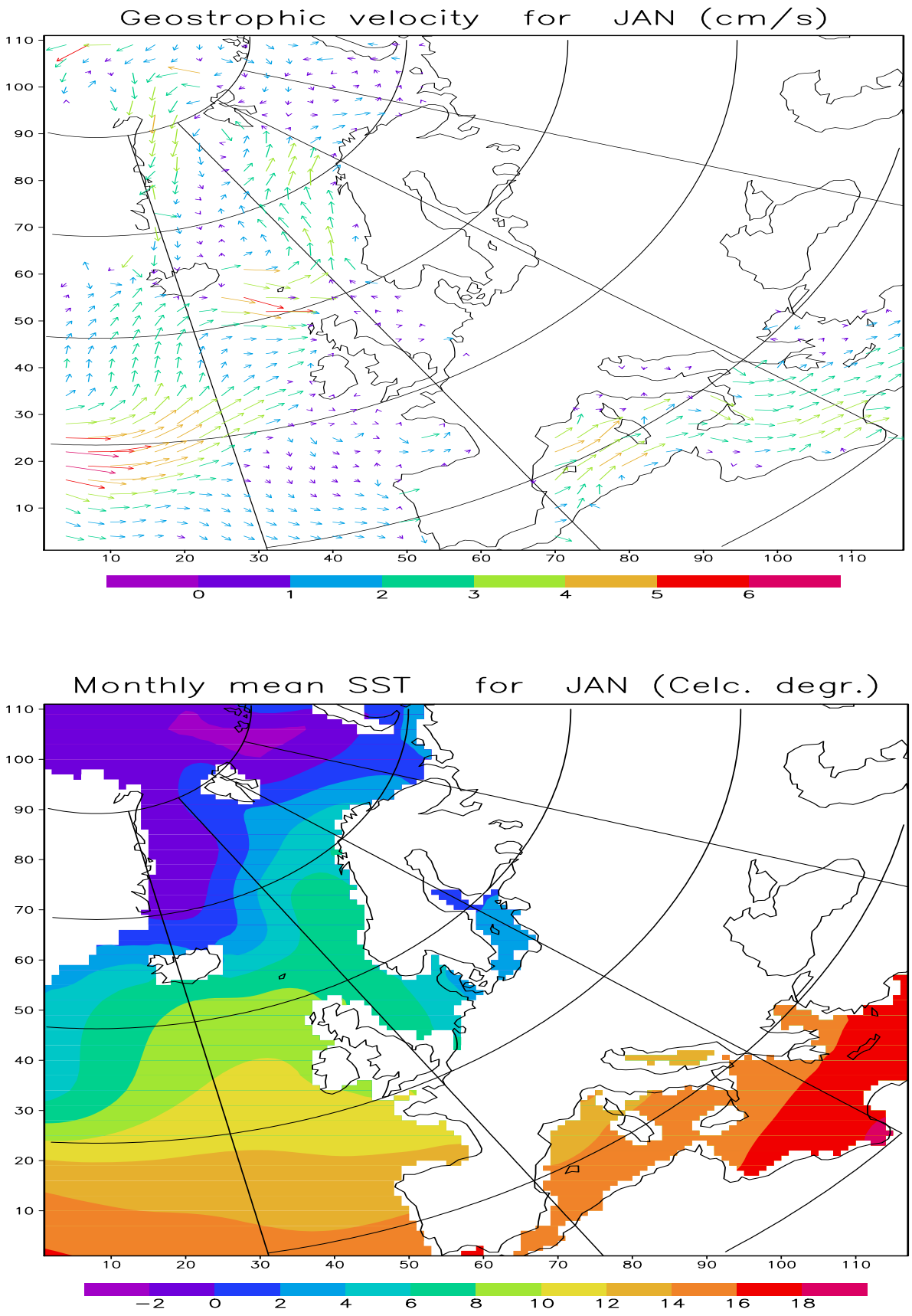

Figure 1 Geostrophic velocity (top, m/s) and
Sea Surface Temperature (SST) (bottom, C^0) in January

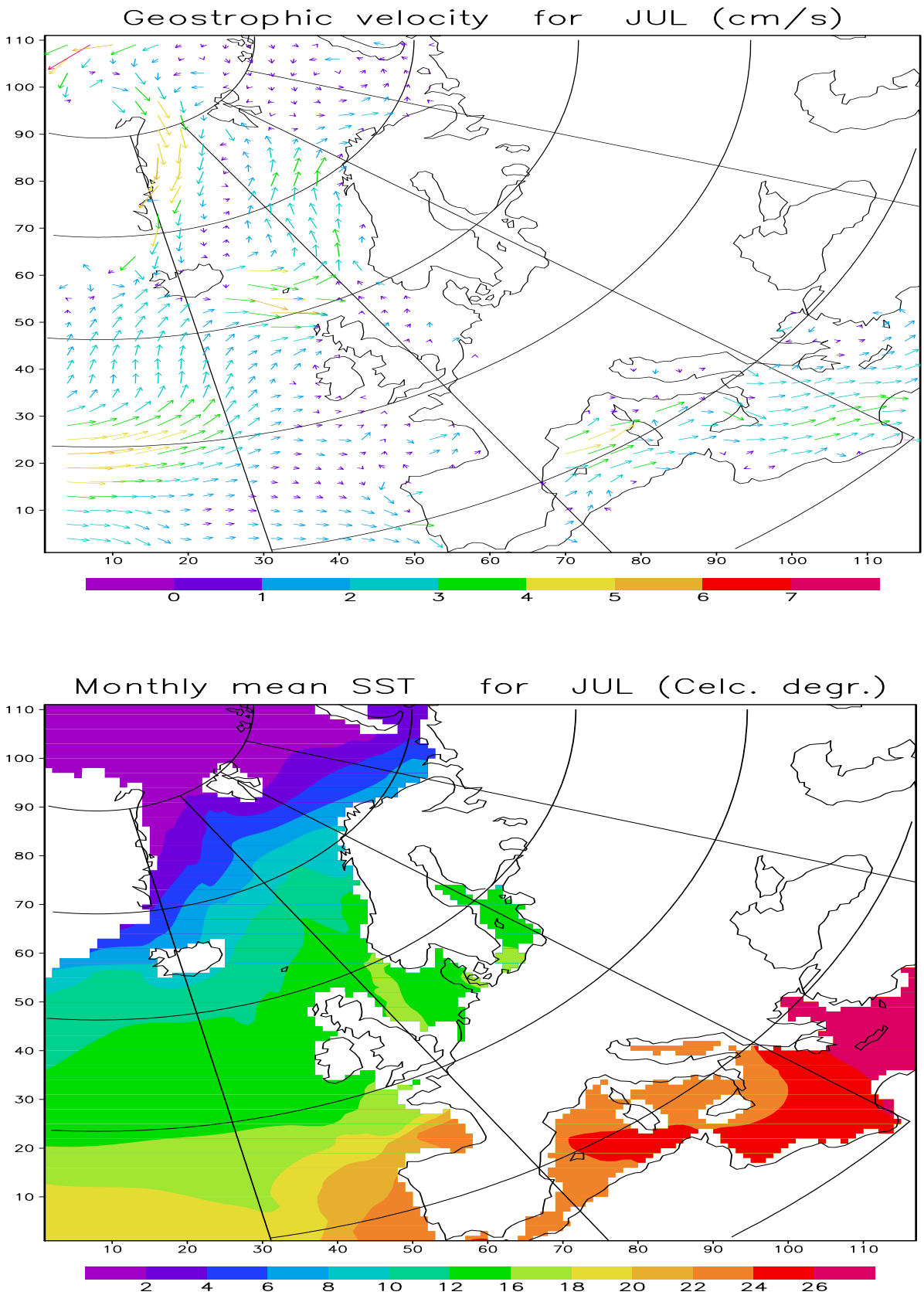

Figure 2 Geostrophic velocity (top, m/s) and
Sea Surface Temperature (SST) (bottom, C^0) in July

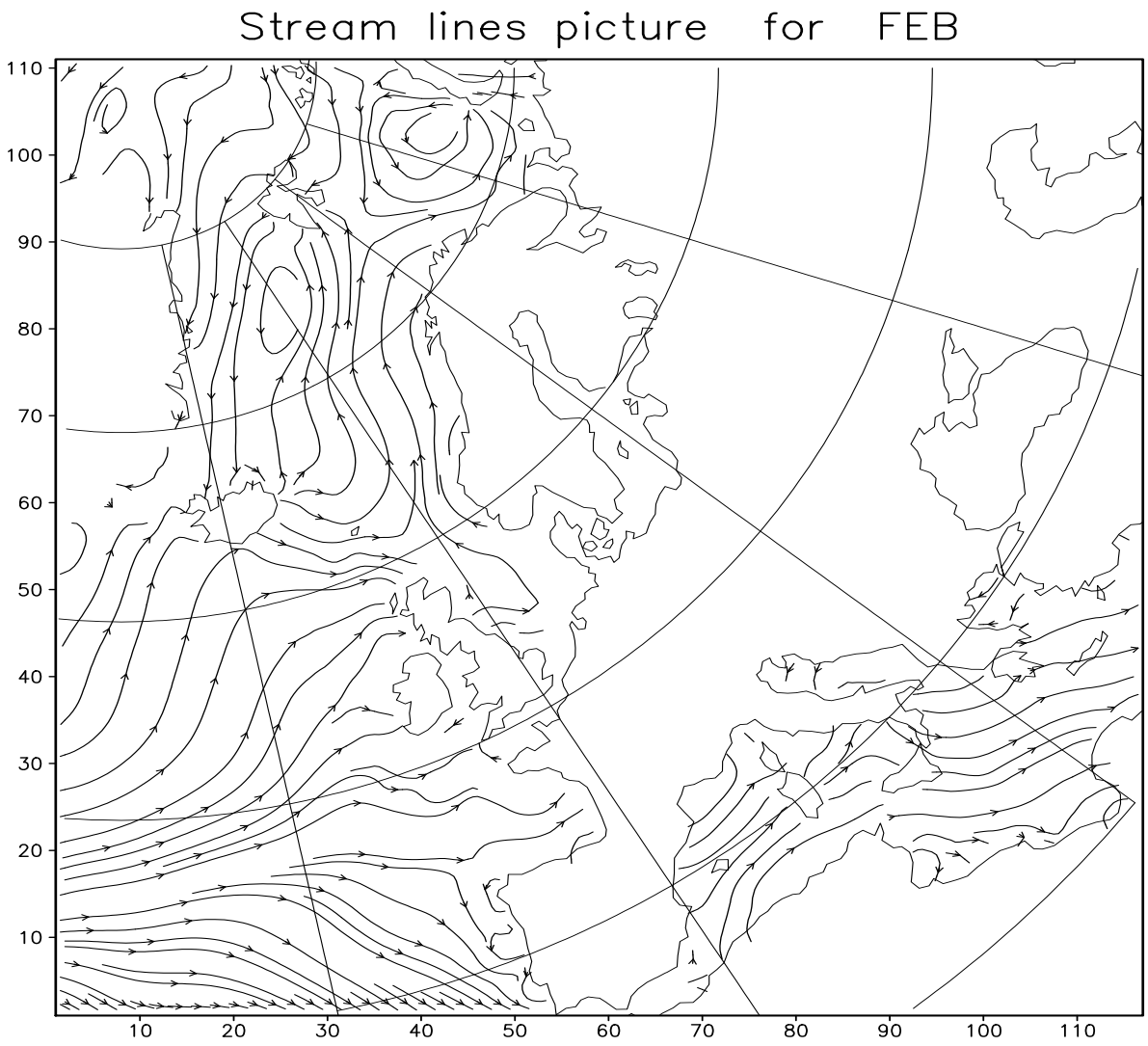

Figure 3 Stream lines picture for February

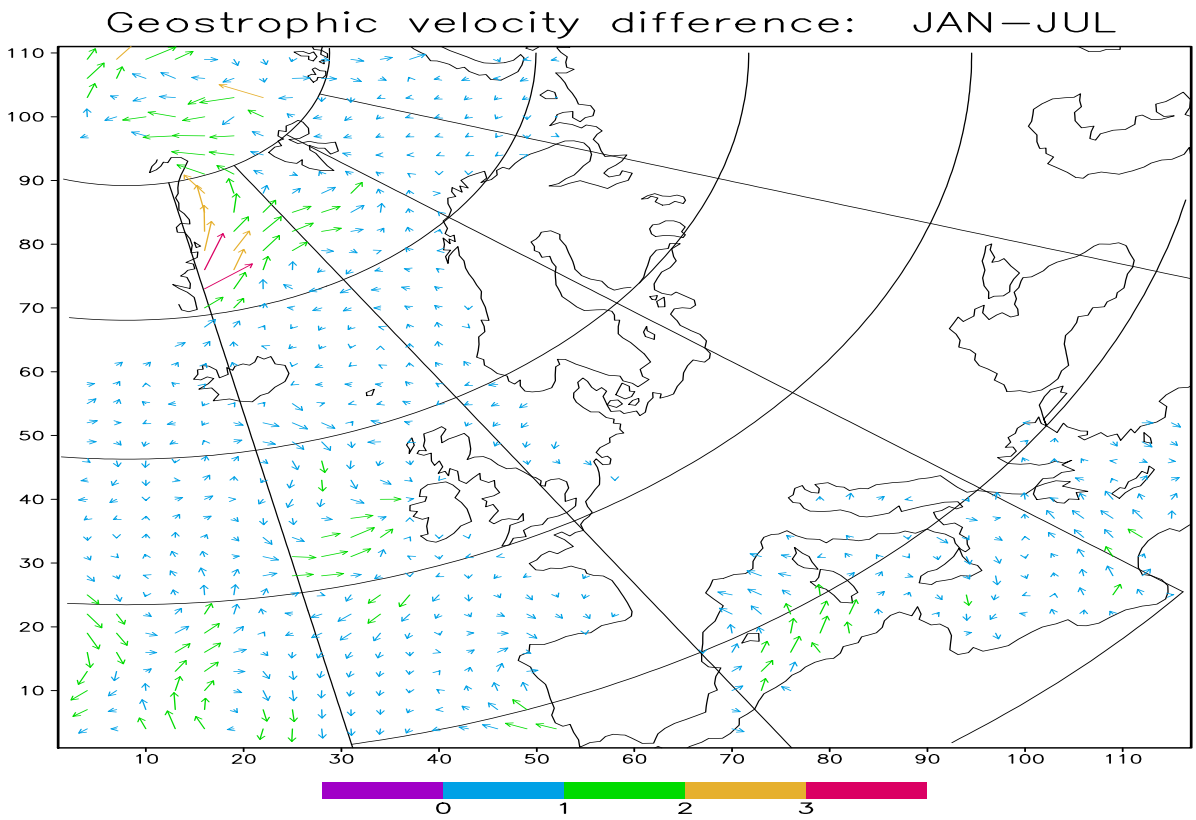

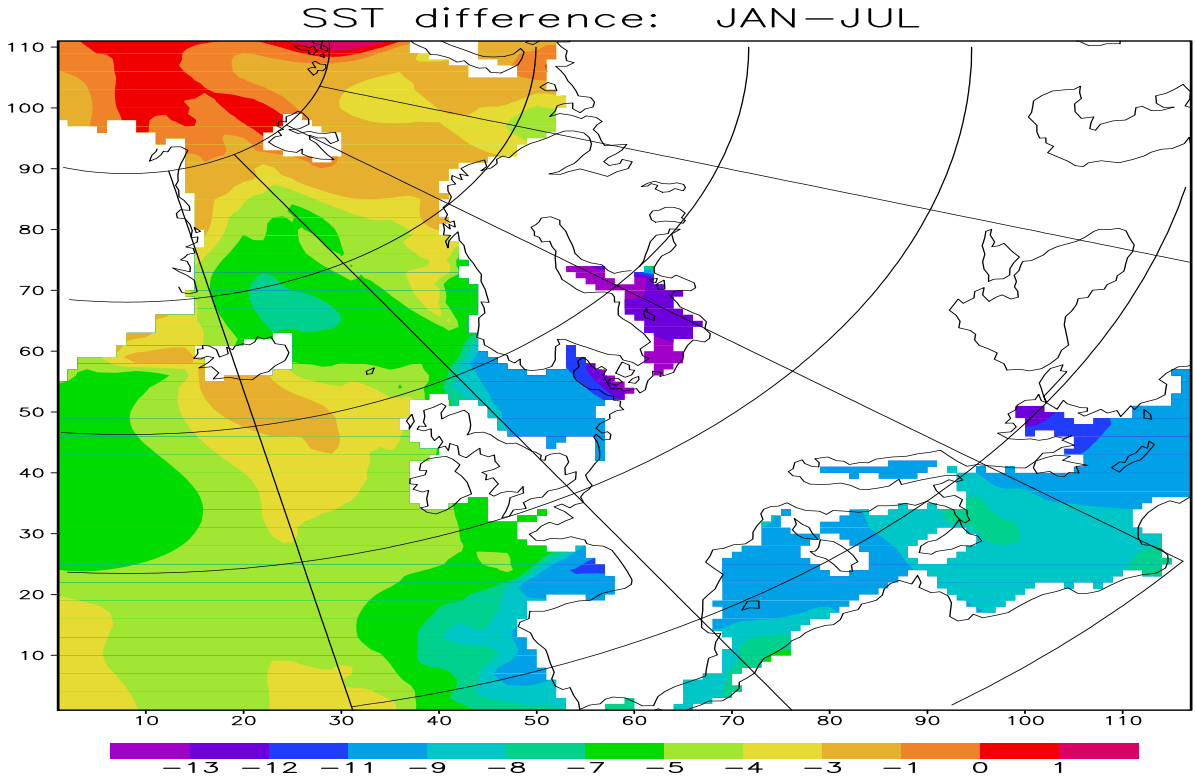

Figure 4 Difference in January-July: geostrophic velocities (top, m/s) and Sea Surface Temperature (bottom, C^0)